Groundwater movement, recharge, and perchlorate occurrence in a faulted alluvial aquifer in California (USA)

By John A. Izbicki, Nicholas F. Teague, Paul B. Hatzinger, J. K. Böhlke, and Neil C. Sturchio

Published in: Hydrogeology Journal, vol. 23, May 2015, p. 467–491

Received: 4 April 2014 /Accepted: 20 November 2014
Published online: 16 December 2014

Electronic supplementary material The online version of this article (doi:10.1007/s10040-014-1217-y) contains supplementary material, which is available to authorized users.

Abstract

Perchlorate from military, industrial, and legacy agricultural sources is present within an alluvial aquifer in the Rialto-Colton groundwater subbasin, 80 km east of Los Angeles, California (USA). The area is extensively faulted, with water-level differences exceeding 60 m across parts of the Rialto-Colton Fault separating the Rialto-Colton and Chino groundwater subbasins. Coupled well-bore flow and depth-dependent water-quality data show decreases in well yield and changes in water chemistry and isotopic composition, reflecting changing aquifer properties and groundwater recharge sources with depth. Perchlorate movement through some wells under unpumped conditions from shallower to deeper layers underlying mapped plumes was as high as 13 kg/year. Water-level maps suggest potential groundwater movement across the Rialto-Colton Fault through an overlying perched aquifer. Upward flow through a well in the Chino subbasin near the Rialto-Colton Fault suggests potential groundwater movement across the fault through permeable layers within partly consolidated deposits at depth. Although potentially important locally, movement of groundwater from the Rialto-Colton subbasin has not resulted in widespread occurrence of perchlorate within the Chino subbasin. Nitrate and perchlorate concentrations at the water table, associated with legacy agricultural fertilizer use, may be underestimated by data from long-screened wells that mix water from different depths within the aquifer.

Introduction

Faults have long been known to influence groundwater flow. Whether faults are impediments or conduits to flow depends on the nature of the faulted material, and the extent and nature of the fault (Freeze and Cherry 1979; Smith et al. 1990; Bredehoeft et al. 1992; Wibberley et al. 2008; Dafny et al. 2013). In bedrock or partly consolidated deposits, faults may be conduits to groundwater flow as a result of fractures within the rock created as movement occurs along the fault. In unconsolidated deposits, faults may be impediments to groundwater flow, as a result of fine-grained material deposited within fractures or clay-rich gouge zones within the fault plane (Caine et al. 2002; Caine and Minor 2009). In alluvial aquifers, fault properties also may differ over short distances and with depth and consolidation of deposits. Faults in older, more-consolidated deposits at depth tend to fracture and may create conduits to groundwater flow. In contrast, faults in younger, less-consolidated deposits may tend to form barriers to groundwater flow. The effect of a fault on groundwater flow may be greater where movement along the fault has been greater and the offset between permeable deposits is greater. In addition, layers of differing permeability within faults may lead to a high degree of anisotropy, with maximum permeability potentially occurring within the plane of the fault (Forster and Evans 1991).

In complex alluvial aquifers, groundwater flow across a fault may be difficult to measure and quantify from field data (Bense et al. 2003; Folch and Mas-Pla 2008). In these settings, flow across a fault is commonly estimated as a residual in groundwater budgets or in numerical groundwater-flow model analyses. It is possible that in areas where groundwater flow across faults is too small to be quantified within regional water budget analyses, these small quantities of groundwater flow may unexpectedly carry contaminants across a fault from one basin to another.

The alluvial deposits that compose the Rialto-Colton groundwater subbasin (California Department of Water Resources 2004), 80 km east of Los Angeles, California (USA), are extensively faulted (Fig. 1). These faults, many of which have little or no surface expression, were first identified as abrupt changes in groundwater-level elevation as great as 120 m in the late 1920s (Eckis 1928; Dutcher and Garrett 1963). Differences in groundwater level elevation associated with these faults were used to define the margins of the groundwater subbasins (California Department of Water Resources 2004).

Perchlorate, an oxidant used as a component of solid rocket fuel, flares, and pyrotechnics, is present in groundwater at sites throughout the United States where perchlorate was manufactured, used, and stored—including many active and former military bases (Brandhuber et al. 2009; Government Accountability Office 2010). Ingestion of perchlorate affects iodine uptake by the human thyroid and thyroidal hormone production (US EPA 2002). Although the US Environmental Protection Agency has not yet established a maximum contaminant level (MCL) for perchlorate in drinking water, California has established a drinking-water perchlorate limit of 6 μg/L (California Department of Public Health 2007).

Perchlorate is highly soluble, moves readily with groundwater, and can be transported great distances in oxic groundwater (Motzer 2001). Microbial degradation of perchlorate can occur in some settings, potentially limiting perchlorate transport in reduced aquifers (Coates and Achenbach 2004; Lieberman and Borden 2008). Knowledge of the distribution and sources of perchlorate in groundwater increased with improved analytical methods and lower detection limits that led to recognition of widespread occurrence of perchlorate in groundwater from agricultural fertilizers derived from nitrate deposits in the Atacama Desert in Chile (Böhlke et al. 2009), and to the identification of low-concentration perchlorate background from natural sources through much of the southwestern United States (Rao et al. 2007; Fram and Belitz 2011). Differences in the chlorine and oxygen isotopic composition of the perchlorate molecule can be used to evaluate perchlorate contributions from different sources (Böhlke et al. 2005; Sturchio et al. 2009 and 2014; Jackson et al. 2010), and to evaluate potential degradation of perchlorate in groundwater under anaerobic conditions (Sturchio et al. 2007a; Hatzinger et al. 2009).

Perchlorate contamination in the Rialto-Colton groundwater subbasin originated in part from military and industrial sources at sites in the northern part of the subbasin (Fig. 1), including the 160-acre site (formerly known as the "BF Goodrich site" and currently known as the "Rockets, Fireworks, and Flares" site; US EPA 2010), and the Former Bunker Site/Mid-Valley Sanitary Landfill (GeoLogic Associates 2003; Woolfenden 2007).

Perchlorate contamination in the area was first identified in 1997, and the mapped extent of perchlorate contamination within two plumes shows perchlorate has moved at least 6 km downgradient from source areas in the general direction of groundwater flow (GeoLogic Associates 2013). Near the source areas, the upgradient portion of the plumes is well defined and perchlorate concentrations in monitoring wells upgradient from and outside of the mapped plume were low or absent during this study. However, there are public-supply wells outside the mapped plumes where perchlorate concentrations have exceeded the California MCL of 6 μg/L, resulting in the removal of these wells from service, or treatment of water from the wells to remove perchlorate. Historical land use data (Lippincott 1902; Wildermuth Environmental Inc. 2000) where military and industrial releases of perchlorate occurred do not show evidence of extensive agricultural land use and concomitant potential for perchlorate associated with legacy agricultural land use that included application of fertilizer from the Atacama Desert. However, perchlorate associated with legacy agricultural land use may be a source of perchlorate elsewhere in the study area, including some areas upgradient and cross gradient of known military and industrial sources (GeoLogic Associates 2002).

The purpose of this study was to evaluate groundwater recharge and movement within the Rialto-Colton subbasin, and the potential for movement of groundwater between the Rialto-Colton subbasin and adjacent Chino subbasin near the northwestern extent of the Rialto-Colton Fault. Scope of the study included: (1) compilation of water-level data and construction of water-level contour maps for selected time periods, (2) collection of chemical and isotopic data from selected wells, (3) collection of coupled well-bore flow, and depth-dependent chemical and isotopic data from selected wells. Data were collected concurrently with samples intended for analyses of the chlorine and oxygen isotopic composition of perchlorate within and near two mapped contaminant plumes within the Rialto-Colton subbasin and from the adjacent Chino subbasin. Results from this study provide the hydrologic framework to support isotopic interpretations of the source(s) of perchlorate in water from wells within the Rialto-Colton and adjacent Chino subbasins.

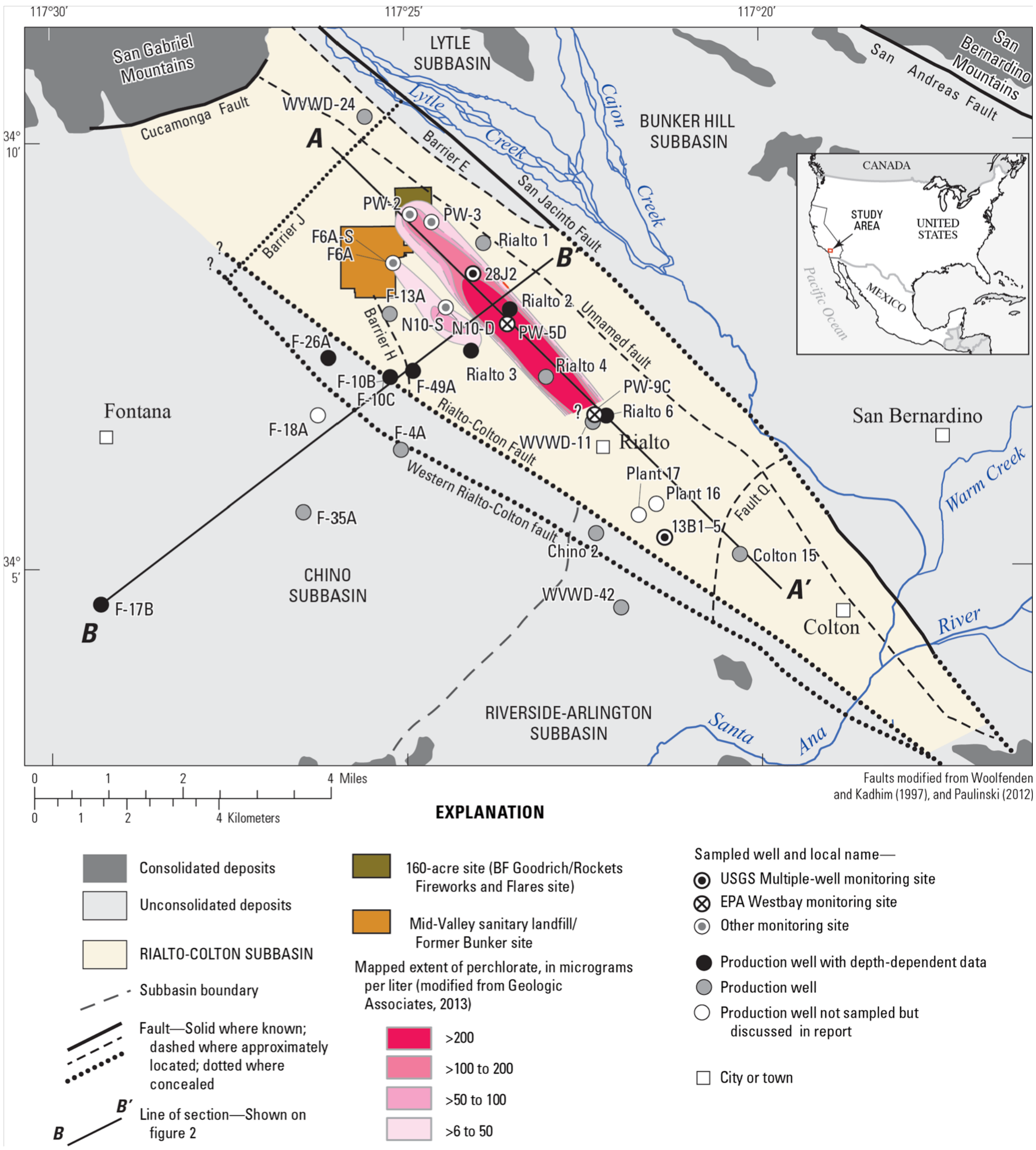

Fig. 1 Location of study area

Hydrogeology

The climate of the study area is Mediterranean, with cool wet winters and hot, dry summers. Average annual precipitation is about 400 mm, and average annual temperature in Rialto, California is about 19 °C. Precipitation is greater and average temperatures lower in the San Gabriel Mountains to the northwest where average annual precipitation, falling mostly during the winter months, exceeds 1,000 mm (Belitz et al. 2004).

In the Rialto-Colton subbasin, unconsolidated alluvial fan deposits of Quaternary age and partly consolidated sedimentary deposits of Tertiary age overlie granitic bedrock (Fig. 2). The upper-most surface of the Tertiary age deposits forms the effective base of the groundwater system (Woolfenden and Kadhim 1997; Woolfenden and Koczot 2001). The overlying alluvial deposits, eroded from the San Gabriel Mountains and deposited by Lytle Creek and other smaller streams, dip to the southeast and range in thickness from about 100 m to slightly more than 240 m (Wisely and Schmidt 2010).

Alluvial deposits within the Rialto-Colton subbasin have been divided into river channel deposits along Warm Creek and the Santa Ana River to the southeast (not shown on section A−A′, Fig. 2), and the regional aquifer has been further subdivided into upper, middle, and lower water-bearing units (Woolfenden and Kadhim 1997; Woolfenden and Koczot 2001; Fig. 2). The deposits dip more steeply than the water table, and the upper water-bearing unit and part of the middle water-bearing unit are unsaturated in the northwestern part of the subbasin (Fig. 2). In this area, a perched aquifer (Fig. 2) overlies low-permeability deposits within the middle water-bearing unit (GeoLogic Associates 1997; GeoSyntec Consultants 2006; Paulinski 2012). To the southeast, additional low permeability deposits separate groundwater within the regional aquifer (Woolfenden 2007). Alluvial deposits within the Rialto-Colton subbasin are extensively pumped for water supply, and the middle water-bearing unit is the primary source of water to wells (Woolfenden and Kadhim 1997). Groundwater pumping increased from about 14.8×10^6 m^3 in 1970 to more than 37×106 m^3 in 2010 (GeoLogic Associates 2010; CH2M-Hill 2012). Since 1998, much of the increase in pumping occurred in the northwestern part of the subbasin. Water levels declined beginning in 1998 in response to increased pumping and decreases in groundwater recharge (CH2M-Hill 2012).

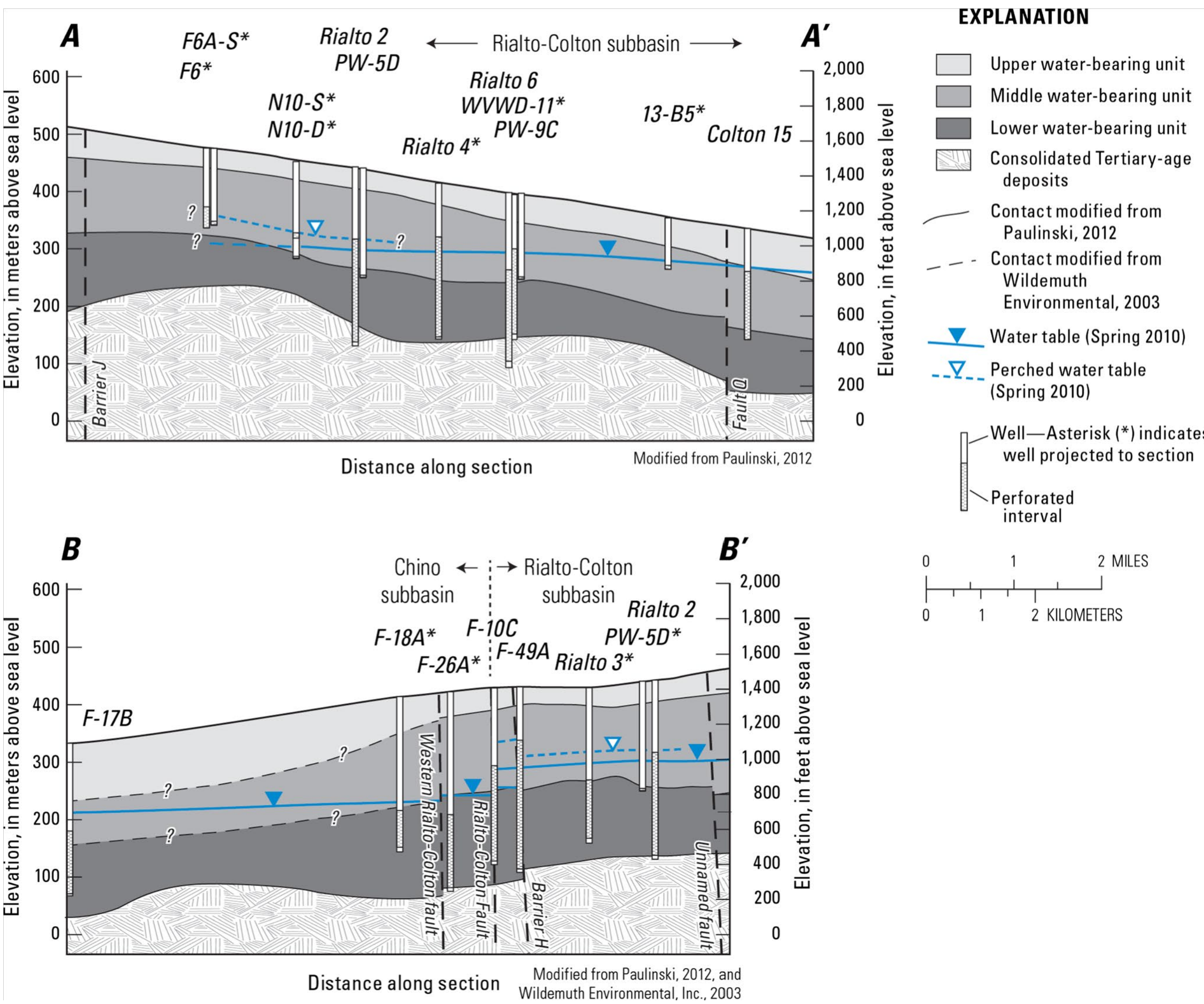

Fig. 2 Sections A–A′ and B–B′ through the Rialto-Colton groundwater subbasin, California

The boundaries of the Rialto-Colton subbasin are defined by the San Jacinto Fault on the northeast, the Rialto-Colton Fault on the southwest, and the San Gabriel Mountains on the northwest (Fig. 1; Dutcher and Garrett 1963; California Department of Water Resources 2004). There is about 25 km of right-lateral offset and 1,000 m of vertical-normal offset along the San Jacinto Fault; and about 2 km of right-lateral offset and 600 m of vertical normal offset along the Rialto-Colton Fault (Wisely and Schmidt 2010). The Rialto-Colton Fault has not ruptured in recent geologic time; consequently, evidence of the fault is not present at the surface, and the depth at which the fault breaks alluvial deposits is not known. Splays of these two larger faults, including Barrier E (Dutcher and Garrett 1963) and an "unnamed fault" (Woolfenden and Kadhim 1997 and Woolfenden and Koczot 2001) have been identified within the subbasin. Barrier H bounds a sediment-filled graben within the underlying Tertiary-age deposits in the northwestern part of the subbasin (Anderson et al. 2004). Collectively these faults generally dip through the alluvium to the east, merging into fewer faults at depth that form a single fault zone within consolidated bedrock (Anderson et al. 2004; Catchings et al. 2008). Locations of individual faults within the Rialto-Colton subbasin and adjacent subbasins are often not precisely known, some faults have been mapped differently by various researchers (Paulinski 2012), and as new information becomes available fault locations may be revised.

Uplift and subsidence occurred as a result of movement along faults, resulting in folding and bending alluvial deposits within the subbasin (Wisely and Schmidt 2010). As a consequence, the upper and middle water-bearing units are not flat-lying (Woolfenden and Kadhim 1997). These units are thicker where subsidence occurred along parts of the San Jacinto Fault between Fault Q and Barrier E, and thinner along parts of the Rialto-Colton Fault between Fault Q and Barrier H (Wisely and Schmidt 2010).

Prior to development and groundwater pumping, recharge to the Rialto-Colton subbasin was from (1) groundwater flow from the Lytle and Bunker Hill subbasins across Barrier E and the San Jacinto Fault, (2) mountain-block recharge from the San Gabriel Mountains (including infiltration from small ungaged streams), (3) areal infiltration of precipitation, and (4) infiltration of streamflow from Warm Creek and the Santa Ana River farther downgradient (Fig. 1; Woolfenden and Koczot 2001). Underflow from the Lytle and Bunker Hill subbasins originated as streamflow infiltrated along the channel of Lytle Creek and its tributaries. Although Lytle Creek is not perennial downstream from the mountains, winter runoff and stormflows may extend along the entire length of its channel to the Santa Ana River. After development, additional recharge also occurred as (1) irrigation return, (2) infiltration of water from stormflow detention basins, and (3) importation of water from northern California (Woolfenden and Koczot 2001).

Groundwater flow is from recharge areas in the northwestern part of the subbasin near the mountain front to discharge areas in the southeast along the Santa Ana River and Warm Creek. The San Jacinto and Rialto-Colton Faults generally restrict groundwater flow along much of their extent. Historically, water-level differences were as much as 15 m across parts of the San Jacinto Fault, and as much as 120 m across parts of the Rialto-Colton Fault (Dutcher and Garrett 1963) in the 1930s. The effect of some faults within the Rialto-Colton subbasin on groundwater movement did not become apparent until after pumping and subsequent water-level declines (GeoLogic Associates 1997, 1998). The Rialto-Colton Fault is not an impediment to groundwater flow in the river channel deposits and in the upper and middle water-bearing units along the southeastern extent of the fault (Gosling 1967; Woolfenden and Koczot 2001). Waterlevel and geophysical data (Gosling 1967), and numerical groundwater flow modeling results (Woolfenden and Koczot 2001) show movement of groundwater from the Rialto-Colton subbasin across the southeastern part of the Rialto-Colton Fault into the adjacent Chino and Arlington groundwater subbasins. On the basis of InSAR data (Lu and Danskin 2001), water-level differences across the Rialto-Colton Fault increase to the northwest toward Barrier H, suggesting that groundwater movement across the fault decreases to the northwest. Groundwater flow across the northwestern part of the Rialto-Colton Fault was simulated as a no-flow boundary in a groundwater flow model of the area (Woolfenden and Koczot 2001).

Recent work showed the San Jacinto and Rialto-Colton Faults to be part of a single fault zone (Anderson et al. 2000, 2004). Anderson et al. (2000, 2004) identified several splays of the Rialto-Colton Fault within bedrock to the west of the Rialto-Colton Fault in the adjacent Chino subbasin, but were unable to determine if those splays extended upward into the alluvium. Catchings et al. (2008) used seismic-reflection data to identify faulting within the alluvium in the Chino subbasin, but did not evaluate the effect of faulting on groundwater flow. Paulinski (2012) suggested that fault splays described by Anderson et al. (2000, 2004) and Catchings et al. (2008) composed a single trace of the larger fault zone running parallel to the Rialto-Colton Fault (Fig. 1). The effect of this "western Rialto-Colton fault" on groundwater flow in the Chino subbasin was not investigated by Paulinski (2012).

Methods

Water-level data

More than 51,800 water-level measurements from 324 wells were obtained from water purveyors and stakeholders in and near the Rialto-Colton subbasin. Data were reviewed for consistency and obvious errors in well location, land-surface elevation, or water-level measurements. Erroneous data were corrected or removed. The data were used to develop water-level maps of the Rialto-Colton subbasin and parts of the Chino and Arlington subbasins (hereafter referred to solely as the Chino subbasin) near the Rialto-Colton Fault for Spring 1996, Spring 2005, and Spring 2010, and for the perched aquifer within the Rialto-Colton subbasin for Spring 2010. The 1996 time period corresponds to the end of model simulations by Woolfenden and Koczot (2001). Water-level hydrographs for selected wells near Barrier H and in the western part of the Chino subbasin were examined.

Field and laboratory methods

Water-quality samples were collected from 17 production wells, 8 monitoring wells, and 2 WestBay sample ports in the Rialto-Colton and adjacent Chino subbasins (Fig. 1; Table 1). Wells were selected to include wells within and outside of the two mapped perchlorate plumes (including upgradient and downgradient wells). Most production wells were sampled from the surface discharge of the existing pump. Monitoring wells were sampled using a 4.5-cm diameter, positive displacement gas-reciprocating pump capable of lifting water from depths greater than 200 m below land surface. Additional samples were collected from WestBay installations using specialized equipment according to manufacturer's specifications.

Table 1 Well-construction, elevation, and depth to water data for sampled wells in the Rialto-Colton and Chino groundwater subbasins, California, June 2010 to February 2012. (Depths in meters below land surface; Elevation in meters above sea level. Mapped plume extent from GeoLogic Associates 2013). *USGS* US Geological Survey

State well number	Local well name	USGS identification No.	Type of well	Depth of well	Depth to bottom of deepest well screen	Depth to top of shallowest well screen	Elevation of land surface datum
Wells in the perched aquifer in the Rialto-Colton subbasin within the mapped plume							
1 N/5 W-28 J2	28 J-2	340828117240102	Monitoring well	137.2	137.2	131.1	460.9
1 N/5 W-29H1	F6	340836117250801	Monitoring well	139.6	139.6	103.0	499.9
1 N/5 W-29H3	F6A-S	340836117250902	Monitoring well	133.2	133.2	127.1	475.5
1 N/5 W-33B2	N-10S	340804117242302	Monitoring well	132.6	132.6	123.4	451.1
Wells in Regional aquifer in the Rialto-Colton subbasin within the mapped plume							
1 N/5 W-21 N2	PW-2	340909117245402	Monitoring well	152.4	150.9	138.7	499.9
1 N/5 W-21P2	PW-3	340904117243502	Monitoring well	152.7	151.2	139.0	487.7
1 N/5 W-33B1	N-10D	340804117242301	Monitoring well	169.5	169.5	166.4	451.1
1 N/5 W-34B2	Rialto 02	340807117232601	Production well	311.5	304.8	179.2	441.7
1 N/5 W-34G4	PW-5D	340752117233104	Westbay port	190.5	190.5	187.5	438.9
1 N/5 W-34 M1	Rialto 03	340218117234601	Production well	270.4	262.1	160.0	429.8
1S/5 W-02B3	PW-9C	340654117222203	Westbay port	149.4	149.4	146.3	396.2
1S/5 W-02G1	Rialto 06	340652117221901	Production well	304.8	292.6	134.1	397.8
1S/5 W-03A1	Rialto 04	340715117230001	Production well	271.3	271.3	93.6	413.6
Wells in the Regional aquifer in the Rialto-Colton subbasin outside the mapped plume							
1 N/5 W-17 K2	WVWD 24	341018117253201	Production well	71.3	67.1	18.3	565.1
1 N/5 W-27D1	Rialto 01	340853117234701	Production well	292.6	292.0	198.1	467.3
1 N/5 W-32A1	F-13A	340759117250801	Production well	304.8	301.8	158.5	456.3
1 N/5 W-33 N1	F-49A	340700117240001	Production well	323.1	317.0	91.4	431.3
1S/4W-18G1	Colton 15	340510117201901	Production well	162.8	162.8	74.4	335.0
1S/5 W-02 K1	WVWD 11	340643117222101	Production well	252.4	239.9	94.5	393.2
1S/5 W-05A5	F-10C	340714117251201	Production well	307.8	301.8	134.1	429.8
1S/5 W-13B5	13B5 (RHSW-5)	340521117212005	Monitoring well	88.4	88.4	82.3	353.6
Wells in the Chino (or Arlington) subbasins							
1S/5 W-04 N1	F-4A	340631117250401	Production well	286.5	280.4	164.6	414.8
1 N/5 W-32 N1	F-26A	340729117260201	Production well	347.5	341.4	213.4	435.9
1S/5W-07R1	F-35A	340541117262401	Production well	259.7	257.6	212.4	380.1
1S/5W-14B1	Chino 02	340525117221901	Production well	222.5	216.4	161.5	362.4
1S/5W-23A1	WVWD 42	340433117215801	Production well	192.0	185.9	106.7	332.2
1S/6W-23D2	F-17B	340438117291402	Production well	265.2	262.1	152.4	332.8

Coupled well-bore flow and depth-dependent water chemistry and isotopic data were collected from seven wells along two sections: one parallel to groundwater flow, and the other perpendicular to groundwater flow that crossed the Rialto-Colton Fault. Well-bore geophysical logs collected from these wells included natural gamma, caliper, fluid temperature, fluid resistivity and electromagnetic (EM) flow logs. Fluid temperature, fluid resistivity, and EM flow logs were collected under unpumped and pumped conditions. Depth-dependent samples were collected under pumped conditions.

Field methods including details of coupled well-bore flow and depth-dependent sample collection (including unpumped and pumped calibration of EM flow logs), sample handling and preservation, laboratory methods, and quality-assurance data are provided in the electronic supplementary material (ESM).

Results and discussion

Water-level data

Regional-scale analysis of water-level data and groundwater flow in the upper Santa Ana River basin was done by Dutcher and Garrett (1963), updated by Gosling (1967), and more recently updated by Wildermuth Environmental Inc. (2000). Water-level maps of the Rialto-Colton subbasin also were prepared as part of geohydrologic and groundwater-flow model studies (Woolfenden and Kadhim 1997; and Woolfenden and Koczot 2001), and as part of perchlorate contaminant studies (GeoLogic 2003; GeoSyntech 2006; DPRA Inc. 2008; CH2MHill 2012). Similarly, water-level maps were prepared as part of groundwater-flow model studies of the Chino subbasin (Wildermuth Environmental Inc. 2003). However, not since Gosling's (1967) work along the southeastern part of the Rialto-Colton Fault, have water-level data been evaluated concurrently on both sides of the Rialto-Colton Fault.

Rialto-Colton and Chino subbasins

Water-level contours for the Rialto-Colton and parts of the adjacent Chino subbasins near the Rialto-Colton Fault are shown for spring 1996, spring 2005, and spring 2010 in Fig. 3a,b,c, respectively. Water levels in both subbasins declined during this period as a result of increased pumping and decreases in recharge. Consistent with previous studies: (1) the direction of groundwater movement in the Rialto-Colton subbasin was toward the southeast, roughly parallel to the faults that bound the subbasin, (2) groundwater movement from the Rialto-Colton subbasin into the Chino and Arlington subbasins occurred across the southeastern part of the Rialto-Colton Fault, and (3) differences in water-levels along the fault increase to the northwest and exceed 60 m in some areas (Fig. 3). The relatively flat gradient in the northeastern part of the Rialto-Colton subbasin is consistent with impediment to areal recharge to the regional aquifer in this area resulting from the overlying low-permeability deposits that form the base of perched aquifer.

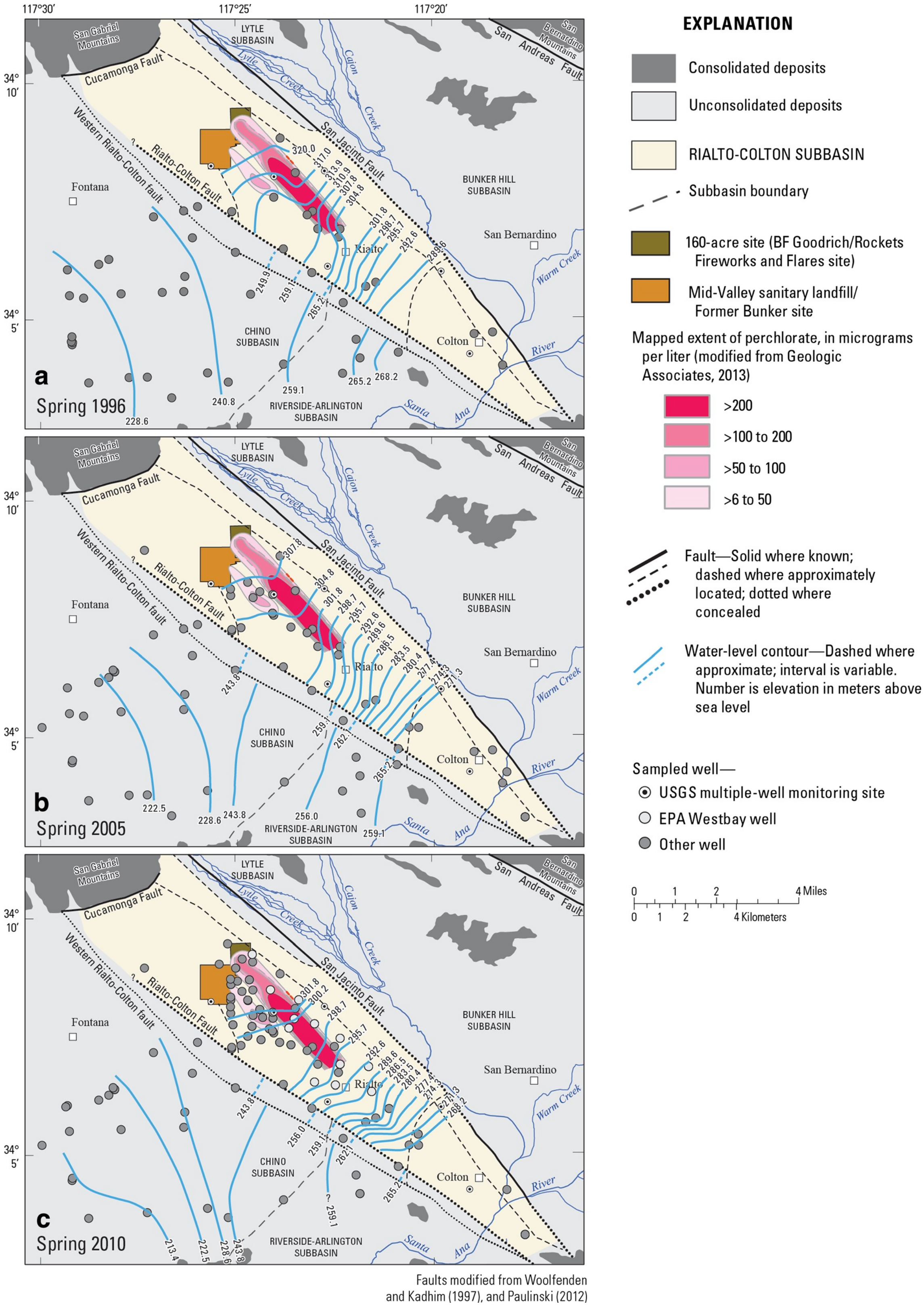

Fig. 3 Water-level contours in the Rialto-Colton and parts of the adjacent Chino groundwater subbasins, California, a Spring 1996, b Spring 2005, and c Spring 2010

Water-level contour maps were constructed largely on the basis of data from production wells screened over long intervals, but also include data from monitoring wells screened over short intervals (USGS multiple-well sites and US EPA WestBay sites). With the exception of the perched aquifer and the underlying

Tertiary-age deposits, differences between water levels in monitoring wells in the regional aquifer in the northwestern part of the subbasin were about 0.3 m. In contrast, vertical differences in water levels in wells at a USGS multiple-well monitoring site in the southern part of the subbasin, 1S/ 3W-13B1-5, were as great as 3 m (Fig. S4 of the ESM). Water levels at this site were lower in wells completed within the middle water-bearing unit as a result of groundwater pumping. Water levels were higher in the well near the water table, and within the underlying Tertiary-age deposits. Similar differences in water levels were observed in production wells screened at different depths within the regional aquifer (Fig. S5 of the ESM). On the basis of these data, water-level contours in the southern part of the Rialto-Colton subbasin (Fig. 3) represent water levels in the main producing zone pumped for water supply, and not necessarily the elevation of the water-table.

Water-level hydrographs from two production wells (F-10C and F49A) in the northwestern part of the Rialto-Colton subbasin along section B–B′ show large declines in recent years (Fig. 4). Between 2000 and 2010, more than half of the pumping from the subbasin was near this area. Water-level declines were greater in well F-10C, between Barrier H and the Rialto-Colton Fault; however, by the early 2000s, water levels in both wells dropped below the bottom elevation of the perched aquifer. Water-level contours for the regional aquifer are not shown between Barrier H and the Rialto-Colton Fault (Fig. 3); however, the interaction between the perched aquifer, the regional aquifer, and the underlying partly-consolidated deposits in this area is examined on the basis of flow-log, chemical, and isotopic data discussed later in this paper.

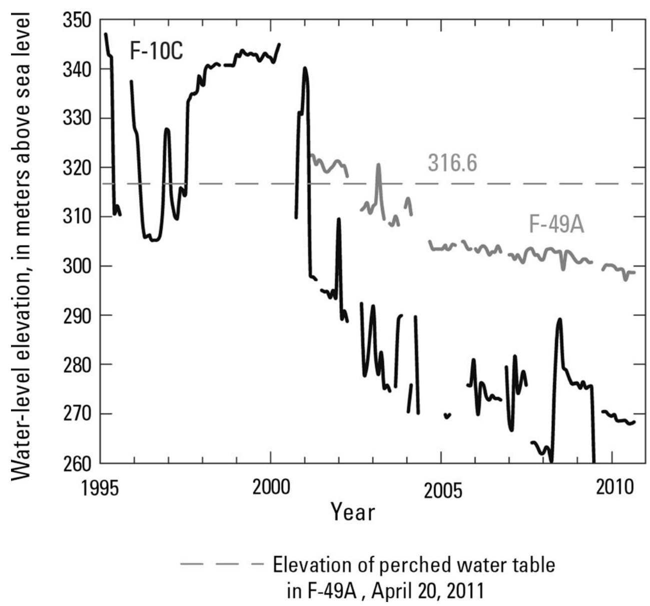

Fig. 4 Water-level hydrographs for wells F-10C (1 N/5 W-5A2) and F-49A (1 N/5 W-33 N1) near Barrier H, Rialto-Colton groundwater subbasin, California, 1995–2010

Water-level contours in the Chino subbasin slope toward the central part of the subbasin (Fig. 3). Water-level data in the Chino subbasin were sparser than data in the Rialto-Colton subbasin and, as a consequence, the contour intervals in the Chino subbasin were larger than in the Rialto-Colton subbasin and intervals differed spatially. Water-level contours in the Chino subbasin assume the “western Rialto-Colton fault” (Paulinski 2012) is an impediment to groundwater flow. This assumption simplified water-level contours—yielding a time-series of maps having a more consistent appearance than maps drawn assuming no effect on water levels from this fault. Water-level hydrographs from wells F4A, F18A, and F35A in the Chino subbasin to the southwest of the “western Rialto-Colton fault” show similar long-term declines in water levels between 1995 and 2010, with declines occurring later in well F4A farther to the southeast (Fig. 5). In contrast, although water levels in wells Chino-2 and F-26A, within fault-bounded alluvium between the “western Rialto-Colton fault” and the Rialto-Colton Fault show declines similar to the other wells, they also show greater response to seasonal pumping (Fig. 5). These data are consistent with compartmentalization of the alluvial deposits by faulting within this area. In some areas, contoured groundwater levels across the “western Rialto-Colton fault” were as much as 6 m higher than water levels in the adjacent parts of the Chino subbasin. In contrast to water-level differences along the Rialto-Colton Fault, difference in water levels along the “western Rialto-Colton fault” decreased to the northwest (Fig. 3). Given the absence of depth-dependent water-level data from monitoring wells, it was not possible to determine how differences in water levels with depth affect contours in the Chino subbasin.

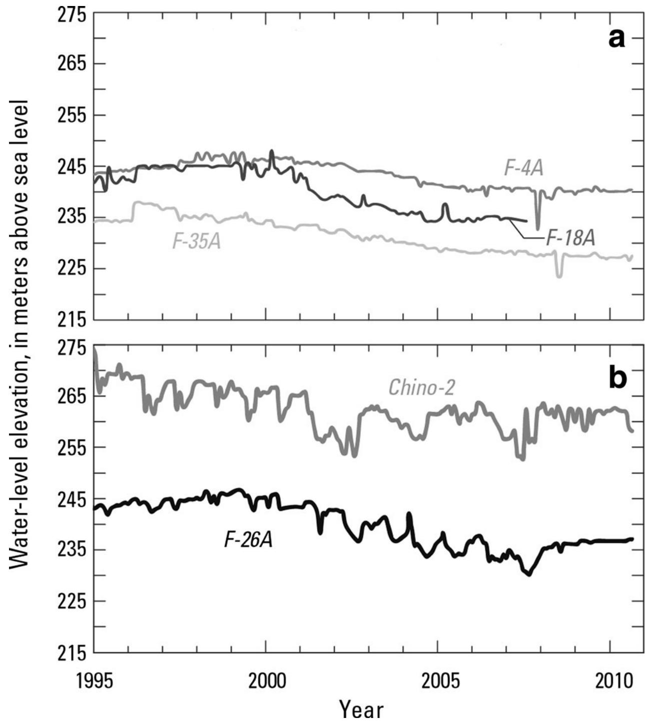

Fig. 5 Water-level hydrographs for wells a F4A, F18A, and F35A, and b Chino-2 and F26A, in the Chino groundwater subbasin, California, 1995–2010

Perched aquifer

Water-level contours for the perched aquifer generally slope to the southeast and the gradient is roughly parallel to the San Jacinto and Rialto-Colton Faults and similar to water levels in the regional aquifer (Fig. 6). Wells completed at different depths within the perched aquifer may have different water levels (GeoLogic Associates 1998); as a result of multiple low-permeability layers within the perched aquifer, or from downward gradients caused by leakance of water through the low-permeability deposits that form the base of the perched aquifer.

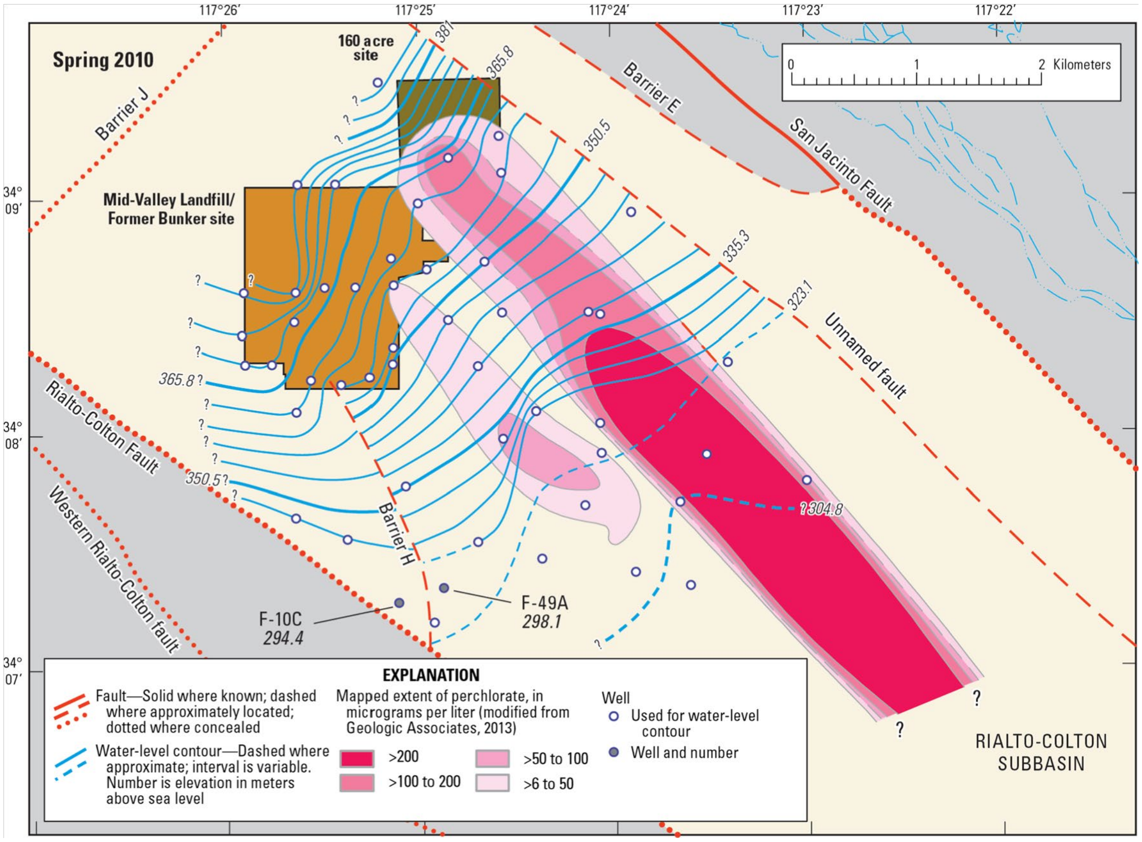

Fig. 6 Water-level contours in the perched aquifer within the Rialto-Colton groundwater subbasin, California, 2010

The Rialto-Colton Fault and Barrier H extend upward into the perched aquifer. During 2010, groundwater flow in the perched aquifer between Barrier H and the Rialto-Colton Fault was to the south, rather than southeast as in the regional aquifer (Fig. 6). This southern direction of flow toward the Rialto-Colton Fault differs from the southeasterly direction of flow previously measured in this part of the perched aquifer (Geologic Associates 1998) prior to the onset of water-level declines from pumping in the underlying regional aquifer beginning in about 2000 (Fig. 4). The Rialto-Colton Fault impedes flow from the perched aquifer into the Chino subbasin, and groundwater levels in the perched aquifer between Barrier H and the Rialto-Colton Fault are higher than levels east of Barrier H (Fig. 6).

Well-bore flow data

Well-bore flow data were collected from seven wells in the Rialto-Colton and Chino subbasins under unpumped and pumped conditions. Two wells (Rialto-2 and Rialto-6) are along section A–A′, aligned in the general direction of groundwater flow, and within the eastern perchlorate plume in the Rialto-Colton subbasin. Six of the wells (F-17B, F-26A, F-10C, F-49A, Rialto-3, and Rialto-2) are along section B–B′; perpendicular to the Rialto-Colton fault and to the general direction of groundwater flow in the Rialto-Colton subbasin (Fig. 1). In addition to flow logs, depth dependent water-chemistry and isotopic data (discussed later in this report) also were collected under pumping conditions from wells along sections A–A′ and B–B′.

Unpumped flow logs

Unpumped flow within a well occurs as a result of differences in water pressure (head) with depth in the aquifer(s) penetrated by the well. Positive values indicate flow in the upward direction; negative values indicate flow in the downward direction; near-zero values (within the $\pm 1\sigma$ precision of the EM flow tool) indicate no flow (Fig. 7). Increasing positive or negative magnitude indicates increasing flow in the upward or downward direction, respectively, as water enters the well from the aquifer. Decreasing positive or negative magnitude indicates decreasing flow as water flows from the well into the aquifer. No change in magnitude indicates water is neither entering nor leaving the well.

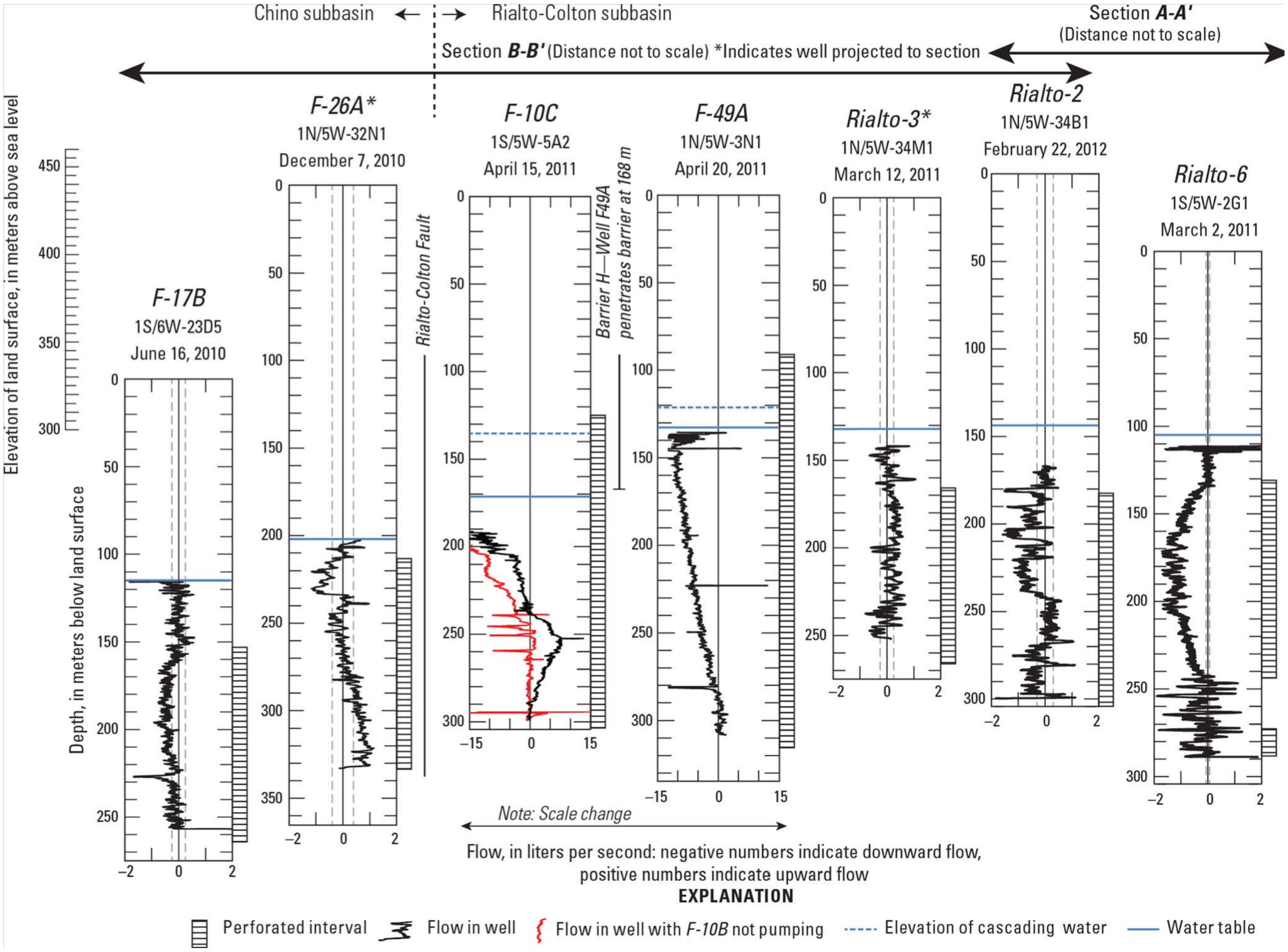

Fig. 7 Unpumped flow logs from selected wells in the Rialto-Colton and Chino groundwater subbasins, California, June 2010 to February 2012

Unpumped flow through wells F-17B and Rialto-6 was downward from the uppermost screens (or perforations) to the major producing zones within the aquifer at rates as high as 0.6 to 1.3 L/s, respectively. The distribution and magnitude of flow within these wells is typical of flow within wells in aquifers pumped for water supply (Fig. 7). In contrast, the magnitude and distribution of unpumped flow through wells F-49A, F-10C, and F-26A, along section B–B′ through Barrier H and the Rialto-Colton Fault, was different as a result of faults, pumping, and cascading water from overlying aquifers (Fig. 7).

Unpumped downward flow was measured at rates as high as 12 and 15 L/s in wells F-49A and F-10C, respectively and water was cascading into the wells from depths of 120.7 m and 136 m below land surface, respectively. (Cascading water was evident on the basis of a roaring sound from within the wells. The depth of the cascade was identified on the basis of fluid temperature and fluid resistivity logs, not shown on Fig. 7.) At the time these data were collected, upward flow at rates as high as 6 L/s also was measured in the deeper parts of well F-10C below 240 m. Downward flow through the upper part of well F-10C and upward flow from the deeper part of the well was redistributed throughout the screened interval into the aquifer as a result of pumping in nearby well F-10B, 60 m to the northeast. After well F10B was turned off overnight (approximately 12 h), downward flow decreased to about 7 L/s and upward flow was reduced to near zero (Fig. 7). Redistribution of flow within well F-49A into the aquifer did not occur in the upper part of the screened interval until a depth of about 168 m below land surface—approximately the elevation of the water table within well F-10C on the opposite side of Barrier H. Below that depth, flow decreased to a depth of about 280 m as water flowed from the well into the aquifer (Fig. 7). The unpumped flow log data suggest well F-49A may be hydraulically connected to the aquifer on the opposite side of Barrier H below a depth of 168 m. Faults in the area are not vertical and generally dip downward through the alluvium to the east (Catchings et al. 2008), and it is possible Barrier H is penetrated by well F-49A at a depth of about 168 m below land surface and lower heads at depth drive flow through well F-49A.

In contrast to wells F-49A and F-10C, upward flow was measured in well F-26A along the section B–B′ on the opposite side of the Rialto-Colton Fault at a rate of about 0.75 L/s (Fig. 7). Flow-log data show water entered the well through a thin interval within the partly consolidated Tertiary-age deposits at a depth of about 326 m below land surface (no flow was measured in the well between 326 m and the bottom of the well at 341 m below land surface), and was redistributed into the aquifer between 325 and 262 m below land surface. Upward flow can occur only if these deeper deposits have a higher head than shallower deposits. It is possible that deposits encountered by well F-26A are hydraulically connected to aquifers having higher head (1) on the opposite side of the Rialto-Colton Fault, about 1,200 m to the east; or (2) on the opposite side of Barrier J, 3 km to the northwest (Fig. 1). If all the flow through well F26A originated as flow across the Rialto-Colton Fault, annual leakance across the fault would be at least 2.4×10^4 m^3—this value is small and less than 0.1 % of the total annual pumpage from the Rialto-Colton subbasin. Because of the small magnitude of leakance and because it may be difficult (or impossible) to identify hydraulically connected layers within complex alluvial aquifers during test drilling prior to installation of traditional short-screened monitoring wells, well-bore flow data from long-screened wells that fully penetrate aquifer deposits may be the only way to identify groundwater flow through hydrologically connected layers across a fault.

Multiple-well monitoring sites completed in partly consolidated Tertiary-age deposits within the Rialto-Colton subbasin commonly have higher water levels than those in the overlying alluvial deposits (Woolfenden and Kadhim 1997; Teague et al. 2014). These differences in water levels may also cause small amounts of upward flow within long-screened wells that penetrate the Tertiary-age deposits. If isolated from sources of recharge, water-level differences between partly consolidated Tertiary-age deposits and overlying alluvium, and resulting well-bore flow, would be expected to dissipate through time and only small amounts of flow would occur through these wells. Consistent with this scenario, only small amounts of upward flow (at rates less than the sensitivity of the flow meter, about 0.1 m/min) were measured in well Rialto-3 within the Rialto-Colton subbasin at distance from faults (Fig. 7). Temperature logs collected within the well (not shown on Fig. 7) were consistent with upward flow through the well. The small rates of upward flow in Rialto-3 would be consistent with flow rates expected solely from partly consolidated deposits at depth that are not hydraulically connected to an aquifer having a higher head.

Pumped flow logs

Pumped flow logs show cumulative flow of water within a well, and identify depth intervals where water enters the well during pumping (Fig. 8). In general, intervals within flow logs that increase in magnitude indicate water entering the well from the aquifer. Greater increases indicate more water entering the well. Vertical intervals indicate little or no water entering the well from the aquifer during pumping.

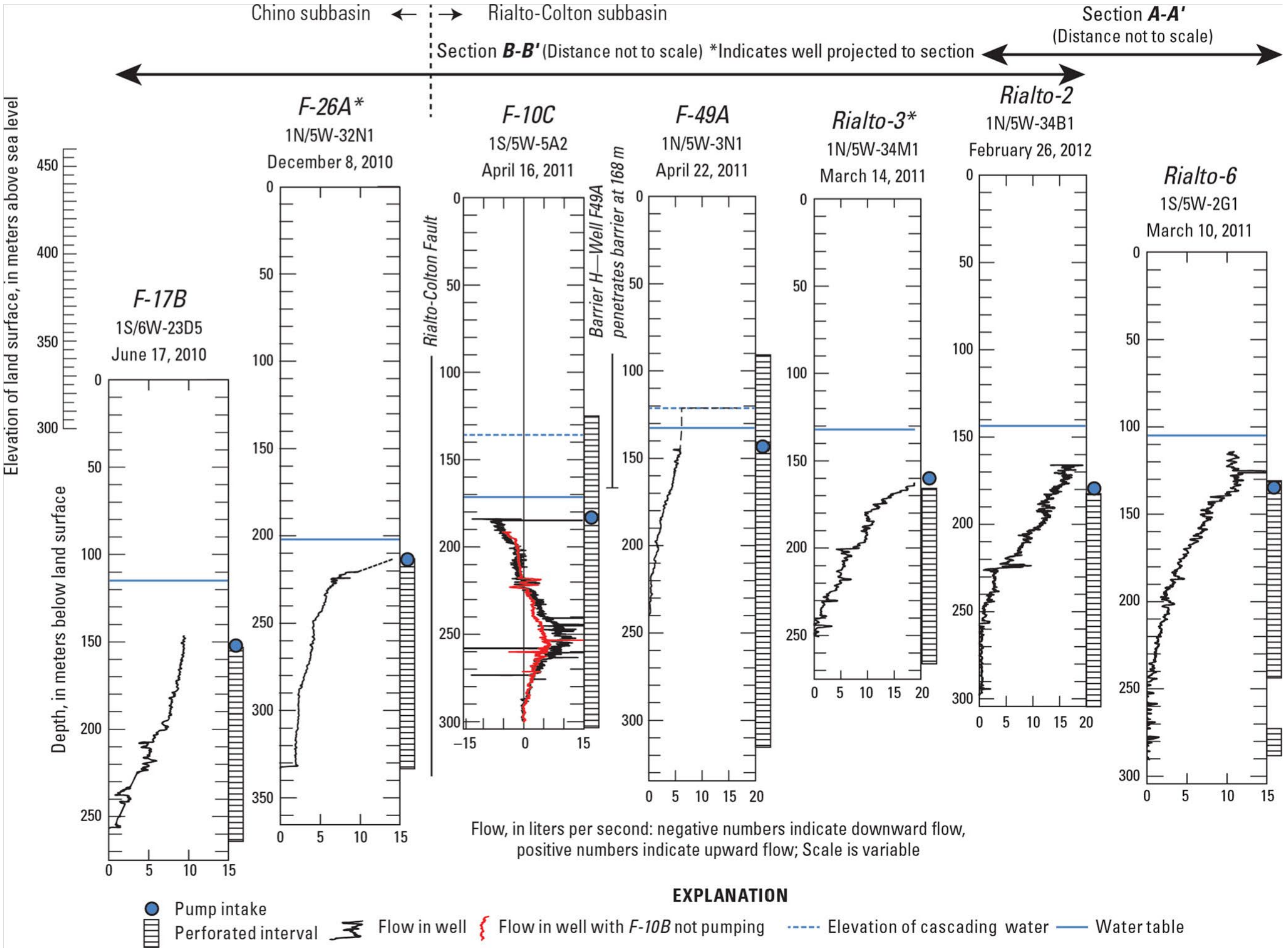

Fig. 8 Pumped flow logs in selected wells in the Rialto-Colton and Chino groundwater subbasins, California, June 2010 to February 2012

Most pumped flow logs in the study show consistently increasing flow from deeper to shallower screens within the well and indicate higher yields from shallower alluvium that contributes as much as 50 % of the flow to some wells (Fig. 8). In general, the logs show changes at depths corresponding to changing hydraulic properties of different aquifer layers (Fig. 8). Assuming the wells are 100 % efficient, these data indicate higher hydraulic conductivities at shallower depths, and lower hydraulic conductivities at deeper depths consistent with finer-grained materials and increasing consolidation with increasing depth (Fig. 8). In contrast to other wells measured, the pumped flow logs from well F-10C show decreasing downward flow from the water table to a depth of about 250 m and upward flow from the bottom of the well as a result of nearby pumping in well F-10 B (Fig. 8).

Changes in flow logs with depth within wells (also fluid conductivity and fluid temperature logs) approximate but do not precisely align with aquifer layers identified previously on the basis of indirect data such as lithologic or geophysical logs (Fig. 9). For example, well-bore flow measured in Rialto-6 under pumped conditions increased at about 140 m below land surface. This increase is consistent with more permeable deposits at that depth, and may indicate the middle water-bearing unit is present to a depth of 140 m below land surface, rather than 121 m previously estimated (Paulinski 2012). Similarly, the low yield to the well below about 243 m is consistent with partly consolidated Tertiary-age deposits at that depth, rather than the 255 m estimated previously. The pumped flow log within the lower water-bearing unit indicates two layers (from 140 to 195 m and 205 to 243 m below land surface) separated by a low-permeability layer (from 195 to 205 m below land surface) that does not contribute water to the well. Each of these features on the flow logs is aligned with changes in the general character of geophysical logs from the well (Fig. 9). This suggests that flow logs (and fluid conductivity and temperature logs), and more commonly collected indirect data such as lithologic or geophysical logs, can be used together to refine conceptual understanding of layering within complex aquifer systems.

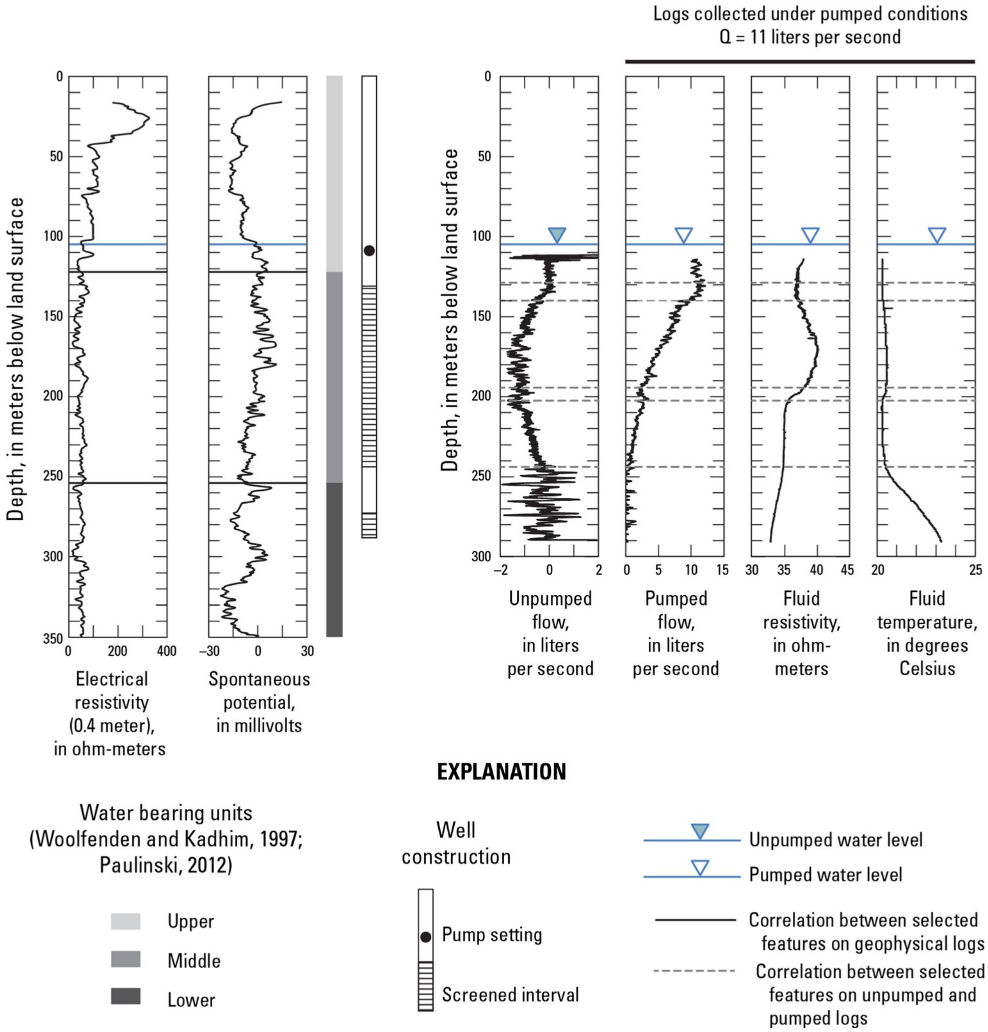

Fig. 9 Selected geophysical and unpumped and pumped well-bore flow logs for well Rialto-6 (1S/5 W-2G1), Rialto-Colton groundwater subbasin, California, March 2011

The utility of flow-log data to refine understanding of aquifer systems is increased when multiple logs are collected along sections through an aquifer so that regional features become apparent (Fig. 8). Similar to Rialto-6, flow logs from Rialto-3, and Rialto-2 show breaks in slope consistent with aquifer layering and changes in hydraulic properties throughout the subbasin. These wells yielded little or no water from deeper parts of the screened interval during pumping, consistent with previous interpretations that the wells penetrate partly consolidated Tertiary-age deposits and the effective base of the aquifer (Paulinski 2012). The depth of the Tertiary-age deposits estimated from flow-log data appears to be shallower than previously suggested (Woolfenden and Koczot 2001; Paulinski 2012). Well F49A penetrates Barrier H and the lack of flow at depths below 240 m may result from well interference associated with nearby pumping in well F-10B between Barrier H and the Rialto-Colton Fault rather than changes in geology. Similarly, nearby pumping in well F-10B obscures correlations with geology in flow-log data collected from well F-10C.

Water-chemistry and isotopic data

Water-chemistry and isotopic data collected from the surface discharge of production wells and from monitoring wells are presented in Tables S1 and S2 of the ESM, respectively. Depth-dependent water-chemistry and isotopic data collected from wells along sections A–A′ and B– B′ during pumped conditions are presented in Tables S3 and S4 of the ESM, respectively. Sample collection depths within wells were determined in the field on the basis of flow-log data (including fluid resistivity and fluid temperature), as discussed in the ESM. The deepest sample within each well is representative of the chemical or isotopic composition of water in the well and the aquifer at the sample depth. The next deepest sample is a mixture of the deepest sample, and water that entered the well between the two sample depths (Izbicki et al. 1999; Izbicki 2004); the shallower samples within a well represent similar mixtures. These mixtures can be resolved on the basis of the pumped flow-log data (see the ESM). In contrast, samples collected near the water table (above the temporary pump) in wells F-10C and F-49A are representative of water at the water table and water from an overlying aquifer cascading into the wells.

Major-ions, perchlorate, and nitrate concentrations

Water from the surface discharge of production wells and from most sampled monitoring wells in the Rialto-Colton and Chino subbasins was oxic and moderately alkaline, with pH ranging from 7.4 to 7.9. In general, dissolved-solids concentrations ranged from 200 to 410 mg/L (Table S1 of the ESM). However, water from two Westbay sample ports sampled within the mapped perchlorate plume, PW-5D and PW-9C, had higher pH values and lower dissolved-solids concentrations (Table S1 of the ESM)—possibly because of their location within the plume, or because of construction and development differences between WestBay wells, production wells, and traditional monitoring wells.

Calcium and bicarbonate were the predominant ions in water from most sampled wells (Fig. 10a). The major-ion composition of water from wells in the perched and regional aquifer within the Rialto-Colton subbasin were generally similar, with small differences in the composition of water from wells F-6 (screened in the perched aquifer adjacent to the Mid-Valley Sanitary Landfill) and 13B5. Although completed in the regional aquifer, monitoring well 13B5 is relatively shallow (screened from 82.3 to 88.4 m below land surface), and reflects water chemistry near the water table (79.2 m below land surface) rather than the larger interval sampled by production wells. Within the regional aquifer, the major-ion composition of water from sampled wells within the mapped plumes was generally similar to the composition of water from wells outside the mapped plumes (with the exception of water from Westbay sample port PW5D discussed previously).

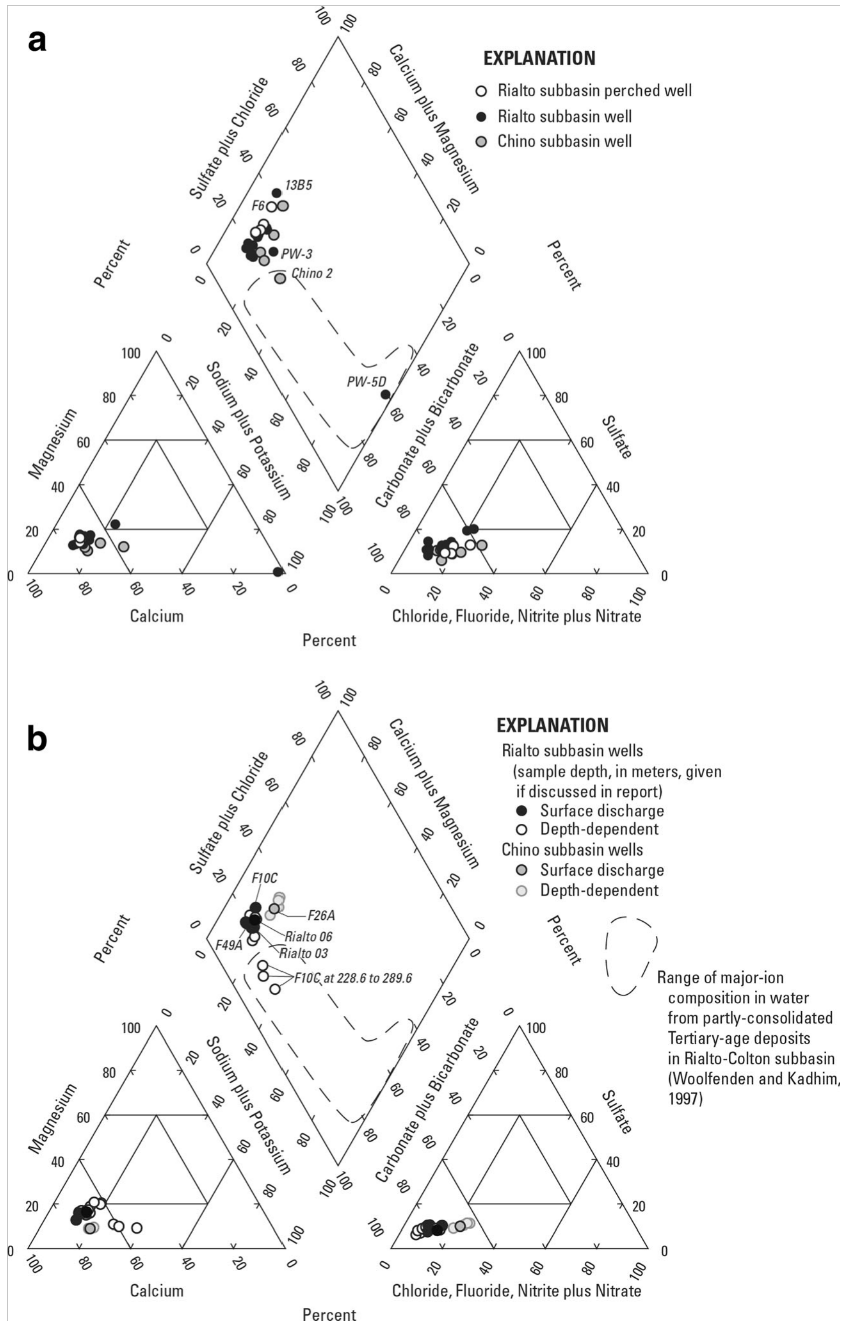

Fig. 10 Trilinear diagram showing the major-ion composition of a water from sampled wells and b depth-dependent samples from selected wells within the Rialto-Colton and Chino groundwater subbasins, California, June 2010 to February 2012

The major-ion composition of water from sampled wells in the Chino subbasin was similar to that of wells in the Rialto-Colton subbasin, with slightly lower calcium plus magnesium fractions, and slightly higher sodium plus potassium percentages in some Chino subbasin samples (Fig. 10a). Water from Chino-2 differed in major-ion composition from most other wells in the Chino subbasin (Fig. 10a). Chino-2 is completed partly in underlying Tertiary-age deposits, and the higher sodium and bicarbonate fractions in water from this well are consistent with the composition of water from the Tertiary-age deposits identified by Woolfenden and Kadhim (1997).

In general, the major-ion composition and dissolved-solids concentration of water from most wells having depth-dependent water-chemistry data were similar to the composition of water from the surface discharge of the well and fairly uniform with depth (Table S3 of the ESM). pH values typically increased with depth, and commonly exceeded 8. Dissolved-oxygen concentrations decreased with depth, and were as low as 0.2 mg/L in water from wells F-10C and Rialto-3, indicative of reducing conditions at depth (Table S3 of the ESM).

In contrast to most sampled wells, the major-ion composition of water at depth within well F-10C, between the Rialto-Colton Fault and Barrier H, differed substantially from the composition of water in the surface discharge of the well (Fig. 10b). At depth, the composition of water was similar to that of water from Chino-2 completed in Tertiary-age deposits underlying the Chino subbasin, and water from Tertiary-age deposits described by Woolfenden and Kadhim (1997; Fig. 10). Given the large quantity of pumping in this area and the complex distribution of flow within well F-10C under unpumped and pumped conditions, large differences in major-ion chemistry with depth are not surprising. The absence of water having a similar major-ion composition within the deeper parts of well F-26A west of the Rialto-Colton Fault might be explained by movement of water from alluvial deposits having higher head on the opposite side of the Rialto-Colton Fault or Barrier J.

Perchlorate concentrations in water from sampled monitoring wells and from the surface discharge of sampled production wells ranged from less than 0.2 to 1,150 μg/L. Perchlorate concentrations were higher in the Rialto-Colton subbasin within the mapped contaminant plumes (Table S1 of the ESM), and were within the range of concentrations measured as part of remedial investigations in the area (US EPA 2004; GeoLogic Associates 2013). Perchlorate concentrations in excess of the California MCL for perchlorate of 6 μg/L were measured in 7 of 14 sampled wells in the Rialto-Colton and Chino subbasins outside the mapped plumes (Table S1 of the ESM). Perchlorate concentrations were as high as 22 μg/L in water from well F-17B in the Chino subbasin farthest from the mapped plumes. The source of perchlorate in water from this well was previously identified as agricultural, rather than synthetic perchlorate, on the basis of its chlorine and oxygen isotopic composition (Sturchio et al. 2007b). Perchlorate concentrations in well F-26 near the Rialto-Colton Fault and Barrier H that had previously exceeded the California MCL of 6 μg/L (Fontana Water District, Fontana Calif., written communication, April 2011) were lower than previously reported, possibly because the well was no longer pumped for supply after perchlorate concentrations in excess of the California MCL were measured.

Along section B–B′ within the mapped plume, perchlorate concentrations near the top of the screened interval in wells Rialto-2 and Rialto-6 (calculated on the basis of flow log and depth-dependent water-quality data; see the ESM) were higher than perchlorate concentrations from the surface discharge from these wells—consistent with a surface source of contamination (Fig. 11). Unpumped flow within these wells was downward (Figs. 7 and 9), allowing redistribution of perchlorate from shallow to deeper aquifer units. The low calculated perchlorate concentrations in Rialto-6 between 171 and 203 m below land surface coincide with the interval where unpumped flow data (Fig. 7) show that water moving downward through the well does not leave or enter the aquifer. Given calculated perchlorate concentrations of 114 and 330 μg/L entering wells Rialto-2 and Rialto-6 from contaminated intervals, respectively (Fig. 11), and measured-downward unpumped flow rates of 1.0 and 1.3 L/s, redistribution of perchlorate through ambient (unpumped) well-bore flow in these wells may be as high as 3.6 and 13 kg/year, respectively. Assuming conditions were similar through time, as much as 130 kg of perchlorate may have moved from shallower to deeper aquifer units through Rialto-6 between the discovery of perchlorate contamination in 2002 and the end of data collection for this study in 2012. Similar redistribution of perchlorate may have occurred through other wells within the mapped plume, and unpumped flow through production wells that are no longer pumped as a result of contamination may partly explain the presence of perchlorate contamination within deeper parts of the aquifer within the Rialto-Colton subbasin that would otherwise be protected from surficial sources of contamination (DPRA Inc. 2008).

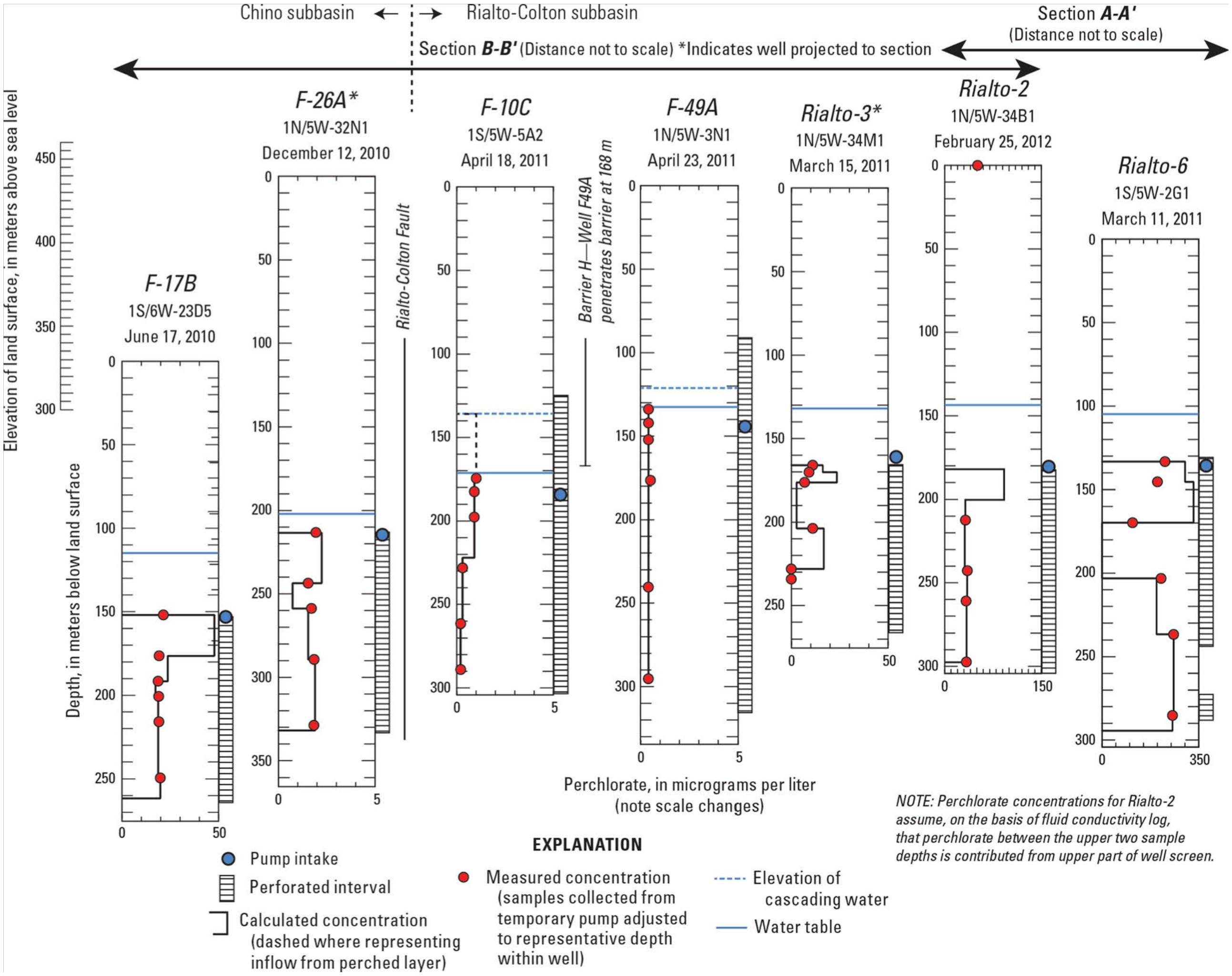

Fig. 11 Depth-dependent perchlorate concentration in water from selected wells, Rialto-Colton and Chino groundwater subbasins, California, June 2010 to February 2012

Perchlorate concentrations also were high throughout well F-17B within the Chino subbasin farthest from the mapped plume. Sturchio et al. (2007b) indicated perchlorate within well F-17B was the result of legacy agriculture and the use of nitrate fertilizer containing perchlorate, rather than military or industrial activities. The perchlorate concentration in the surface discharge from well F-17B was 22 µg/L (Tables S1 and S3 of the ESM); whereas, the calculated perchlorate concentration from the uppermost part of the well screens (between 152.4 and 176.8 m depth, Table S3 of the ESM) was 47 µg/L (Fig. 11).

Although subject to some uncertainty, these data illustrate how samples from the surface discharge of production wells, screened over long intervals, yield mixtures of water having different perchlorate concentrations from different depths within an aquifer. Interpretation of data from long-screened wells may underestimate maximum perchlorate concentrations near the water table associated with legacy agricultural use of fertilizer in the Chino subbasin. Similar to wells Rialto-2 and Rialto-6, downward flow through well F-17B under unpumped conditions also may be responsible for perchlorate in deeper parts of the aquifer. Given a concentration of 47 mg/L (Fig. 11) and unpumped downward flow at a rate of 0.6 L/ s (Figs. 7 and 9), redistribution of perchlorate from legacy agriculture through well F-17B may be as high as 0.9 kg/ year.

The perchlorate concentration in the surface discharge of well F-26A was about 2 µg/L. Depth-dependent water-quality data indicate two layers of water containing perchlorate within the well—a shallow layer from the water table to a depth of about 244 below land surface, and a deeper layer from 262 to 326 to about m below land surface (Fig. 11). Perchlorate at shallower depths may have originated from legacy agricultural land uses in this area (Lippincott 1902; Wildermuth Environmental, Inc. 2000) similar to perchlorate in well

F-17B. Perchlorate at deeper depths also may have legacy agricultural source or from other sources associated with water that flowed through the perched aquifer across the Rialto-Colton Fault (Fig. 6). However, perchlorate concentrations within the perched or regional aquifer in the Rialto-Colton subbasin west of the mapped plumes during this study were less than 1 µg/L and not high enough to explain concentrations as high as 6 µg/L in water from well F-26A. Unpumped flow data (Fig. 7) show perchlorate at depth originated with water that entered the well between 315.5 and 330.7 m below land surface. Unpumped flow within this part of the well was upward (Fig. 7), and unlike wells Rialto-2, Rialto-6, and F-17B perchlorate at depth within well F-26A is not the result of redistribution from shallow depths within the well under unpumped conditions. As previously discussed, upward flow within well F-26A may be driven by aquifers having higher head (1) on the opposite side of the Rialto-Colton Fault, about 1,200 m to the east, or (2) on the opposite side of Barrier J, 3 km to the northwest (Fig. 1).

Perchlorate concentrations in the surface discharge from wells F-10C, and F-49A were low, 0.93 and 0.43 µg/L, respectively (Fig. 11, Table S3 of the ESM). Comparatively uniform perchlorate concentrations in the upper part of well F-10C to a depth of 198 m and throughout well F-49A (ranging from 0.9 to 1.0 and 0.4 to 0.5 µg/L, respectively) are consistent with redistribution of water and perchlorate throughout the wells under unpumped conditions (Fig. 7). Lower concentrations of perchlorate at depth in well F-10C, ranging from 0.2 to 0.3 µg/L (Table S3 of the ESM) detected using ionchromatography mass-spectrometry (ICMS), in water having a major-ion composition similar water from Tertiary-age deposits (Fig. 10b) could be consistent with low natural perchlorate background concentrations in groundwater in the southwestern United States (Rao et al. 2007; Fram and Belitz 2011).

Nitrate concentrations in water from sampled monitoring wells and from the surface discharge of sampled production wells ranged from 1.6 to 14.8 mg/L as nitrogen (mg/L as N; Table S1 of the ESM). Concentrations were higher outside the mapped plume boundaries, and water from three sampled wells (13B5, F-4A, and F-17B) exceeded the MCL of nitrate of 10 mg/L as N. Nitrate and perchlorate were not significantly correlated (on the basis of Kendall's Tau correlation coefficient with a confidence criteria of α=0.05). This differs from results in the nearby Bunker Hill subbasin where nitrate and perchlorate were positively correlated (Kent and Landon 2012), consistent with a legacy agricultural source of perchlorate.

Nitrate was present at detectable concentrations in all depth-dependent samples within sampled wells, even in samples where perchlorate was not detected (Table S4 of the ESM). Although nitrate and perchlorate were not highly correlated overall, the distribution of nitrate and perchlorate in depth-dependent samples was similar and nitrate data also showed effects of redistribution from surface sources of contamination through wells (Fig. 12). Similar to perchlorate, calculated nitrate concentrations of 32 mg/L as N in water from near the top of the screened interval in well F17B were higher than the concentration in the surface discharge from the well of 14 mg/L as N (Fig. 12), and indicate the potential for data from long-screened production wells to underestimate maximum nitrate concentrations associated with legacy agricultural fertilizer use.

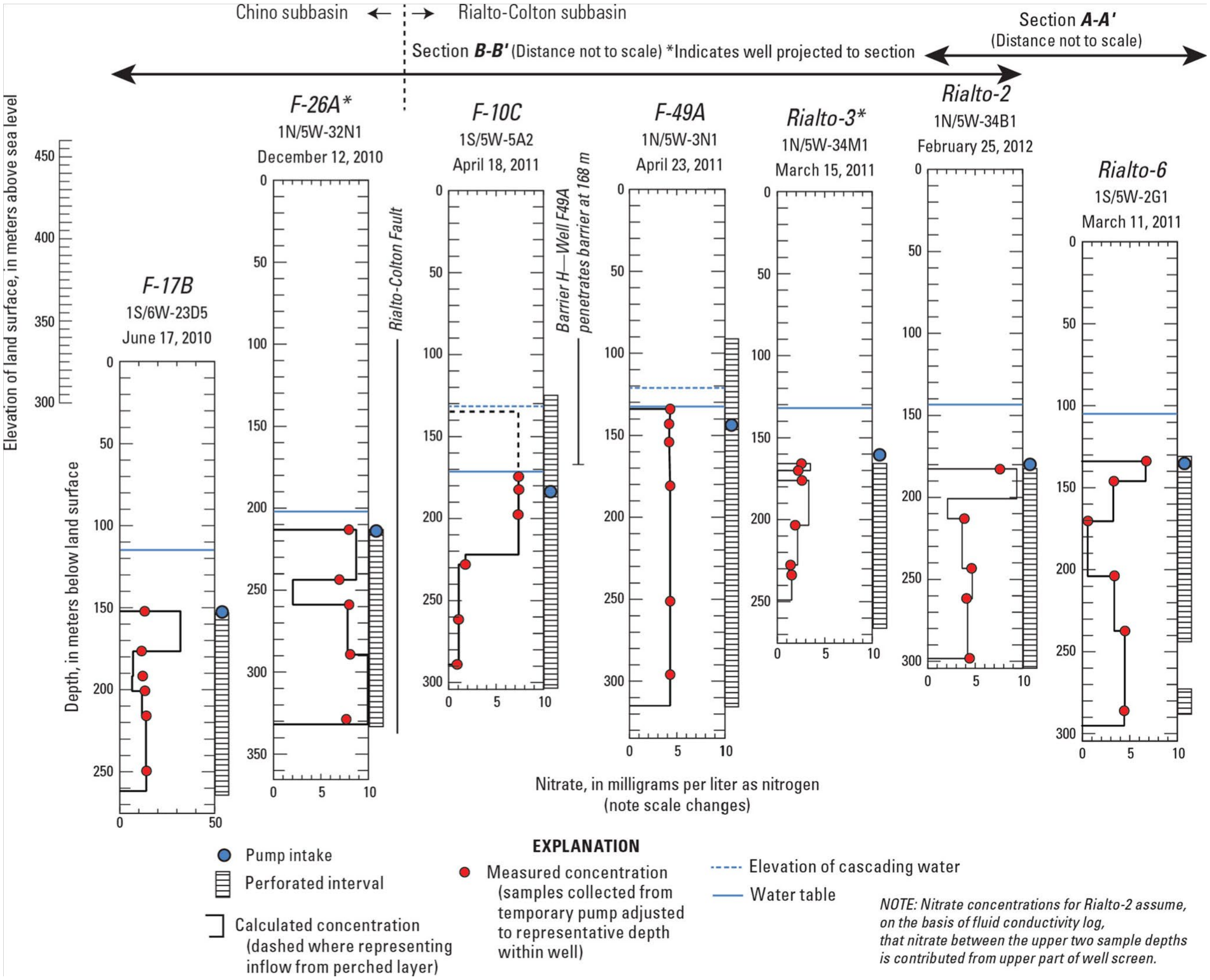

Fig. 12 Depth-dependent nitrate concentration in water from selected wells, Rialto-Colton and Chino groundwater subbasins, California, June 2010 to February 2012

Stable oxygen and hydrogen isotope ratios in water

The stable oxygen and hydrogen isotope ratios (reported in delta notation as $\delta^{18}O$ and $\delta^{2}H$, respectively) in precipitation throughout the world are linearly correlated and distributed along a line known as the Global Meteoric Water Line (Craig 1961). Water that condensed and precipitated in cooler environments at higher altitudes typically contains less of the heavier isotopes (has more negative delta values) and is isotopically lighter than water that condensed in warmer environments at lower altitudes (which has less negative delta values and is isotopically heavier). In addition, water that has been partly evaporated contains more of the heavier isotopes and is shifted to the right of the meteoric water line along an evaporative trend line as a result of preferential removal of lighter isotopes (IAEA 1981).

The $\delta^{18}O$ and $\delta^{2}H$ values of water from the surface discharge of sampled production wells and monitoring wells ranged from −9.5 to −7.6 and −62 to −50 ‰, respectively (Table S2 of the ESM)—and was similar to the isotopic compositions in water from wells in the study area sampled by Woolfenden and Kadhim (1997) and Teague et al. (2014). Most samples from the Rialto-Colton subbasin plot along a local groundwater line about 3 ‰ (with respect to δ2H) above the Global Meteoric Water Line (Fig. 13a)—consistent with previous work that showed precipitation and groundwater in the San Gabriel and San Bernardino Mountains near Cajon Pass has $\delta^{2}H$ values about 3 ‰ above the Global Meteoric Water line (Izbicki et al. 1998; Izbicki 2003; Woolfenden and Kadhim 1997).

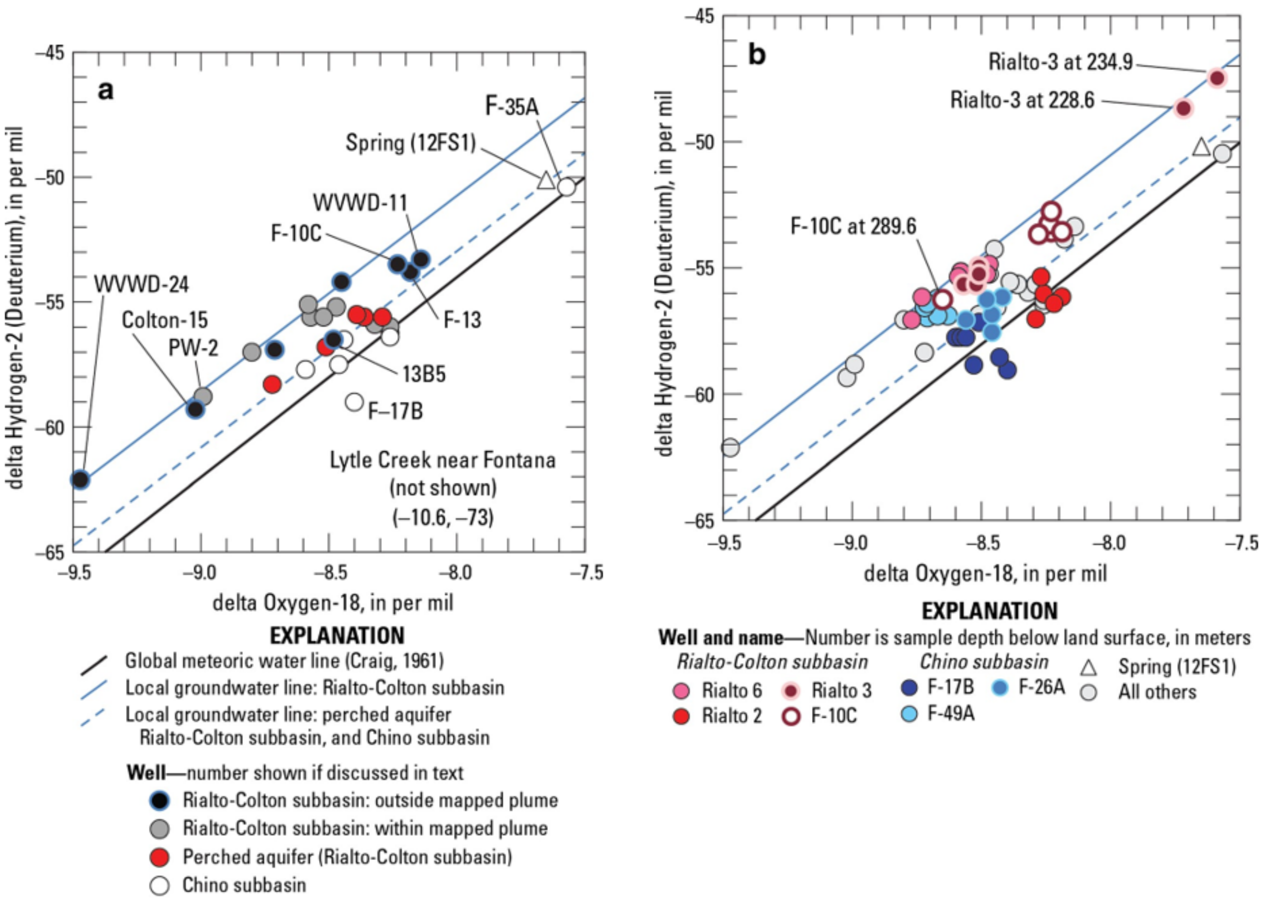

Fig. 13 Stable oxygen and hydrogen isotope ratios—delta Oxygen-18 (δ18O) and delta Hydrogen-2 (δ2H) respectively—in water a from sampled wells, and b depth-dependent samples from selected wells in the Rialto-Colton and Chino groundwater subbasins, California, June2010 to February 2012

Lytle Creek drains the higher altitudes of the San Gabriel Mountains immediately west of Cajon Pass (Fig. 1) and is an important source of recharge to the Rialto-Colton subbasin. Although the isotopic composition of streamflow in Lytle Creek probably varies widely, a sample collected from Lytle Creek by Woolfenden and Kadhim (1997) had relatively light $\delta^{18}O$ and $\delta^{2}H$ values of −10.6 and −73 ‰, consistent with precipitation and runoff from higher altitudes. Groundwater samples with similarly light $\delta^{18}O$ and $\delta^{2}H$ values consistent with a high fraction of recharge from Lytle Creek include water from well WVWD-24 upgradient from the mapped perchlorate plume, and water from well PW-2 near the northeastern edge of the perchlorate plume (Fig. 13a). Water from well Colton-15, farther from the mountain front in the southeastern part of the Rialto-Colton subbasin, also was isotopically light and may contain a high fraction of recharge from Lytle Creek or another other high altitude source (Fig. 13a).

In contrast, recharge from precipitation at lower altitudes along the front of the San Gabriel Mountains had less negative $\delta^{18}O$ and $\delta^{2}H$ values. For example, a spring (12FS1) sampled by Woolfenden and Kadhim (1997) near the front of the San Gabriel Mountains had $\delta^{18}O$ and $\delta^{2}H$ values of −7.7 and −50 ‰, respectively (Fig. 13a). Water from wells F-10C, and F-13A, farther from Lytle Creek, was isotopically heavier than water from most other sampled wells, plots slightly below the local groundwater line, and may contain a high fraction of recharge from lower altitude sources along the front of the San Gabriel Mountains.

Water from wells in the perched aquifer in the Rialto-Colton subbasin plot along a line about 1 ‰ above the Global Meteoric Water Line and have only a small range in $\delta^{18}O$ and $\delta^{2}H$ values intermediate between higher altitude and lower altitude recharge sources (Fig. 13a). Most samples from the Chino subbasin, farther from Cajon Pass, also plot closer to the Global Meteoric Water Line than samples from the regional aquifer within the Rialto-Colton subbasin. The $\delta^{18}O$ and $\delta^{2}H$ values of water from well F-35A in the Chino subbasin were heavier and similar to those of water from the mountain front spring, despite the locations of well F-35A comparatively far from the mountain front within the Chino subbasin. Water from well F17-B, farthest from the mapped perchlorate plume, is the only well that plots below the Global Meteoric Water Line (Fig. 13a), possibly consistent with partial evaporation of irrigation return water associated with legacy agriculture.

The $\delta^{18}O$ and $\delta^{2}H$ values of depth-dependent samples from most wells were fairly similar with depth, typically having a range of less than 3 ‰ with respect to $\delta^{2}H$ (Table S4 of the ESM). The largest range in $\delta^{2}H$ values in depth-dependent samples within a well, 8 ‰, was from well Rialto-3 (Fig. 13b). The deeper samples from this well (228.6 and 234.7 m below land surface) were isotopically heavier and similar in composition to water recharged along the front of the San Gabriel Mountains; the shallower samples were isotopically lighter and similar to water recharged from Lytle Creek (Fig. 13a,b). These data show water recharged from different sources can flow along discrete flowpaths through the aquifer with depth. As a consequence, the sources and quantity of water recharged from the mountain front may be difficult to characterize solely on the basis of samples collected from the surface discharge of wells. A range of about 3 ‰ in $\delta^{2}H$ values was present in water from well F-10C (Fig. 13b). In contrast to Rialto-3, the deepest sample from F-10C (289.6 m below land surface) was isotopically lighter than water from shallower samples (Table S4 of the ESM). Major-ion data, discussed previously (Fig. 11a), are consistent with water from Tertiary-age deposits and with age-dating parameters (discussed in the next section) that show this is among the oldest water sampled as part of this study.

Age-dating parameters

Tritium (^{3}H) is a naturally occurring, radioactive isotope of hydrogen having a half-life of about 12.3 years. Tritium is measured as an activity, in picoCuries per liter (pCi/L). One picoCurie is about 0.037 atomic disintegrations per second. For the purposes of this report, samples that do not contain measurable tritium are interpreted as groundwater recharged prior to 1952, and samples containing tritium are interpreted as groundwater containing at least some fraction of water recharged after 1952. Tritium may provide information relevant to the source and occurrence of perchlorate. Most perchlorate associated with agricultural use of Chilean nitrate fertilizer would likely have been introduced prior to World War II, and most synthetic perchlorate associated with military or industrial sources would largely have been introduced after World War II (Böhlke et al. 2009; Sturchio et al. 2009; Brandhuber et al. 2009; Government Accountability Office 2010).

Tritium activities in water from the surface discharge of wells in the Rialto-Colton subbasin ranged from 1.0 to 8.6 pCi/L (Table S2 of the ESM). Tritium activities were higher in the perched aquifer than in the regional aquifer (Fig. 14). Within the regional aquifer, tritium activities decreased from recharge areas in the northeastern part of the study area near sources of perchlorate contamination downgradient to Rialto-6 and WVWD-11, near the leading edge of the mapped perchlorate plume. Tritium activities were slightly higher farther downgradient in well Colton-15, where $\delta^{18}O$ and $\delta^{2}H$ data (Fig. 13) indicate recharge from infiltration along downstream reaches of Lytle Creek near the leading edge of the mapped perchlorate plume.

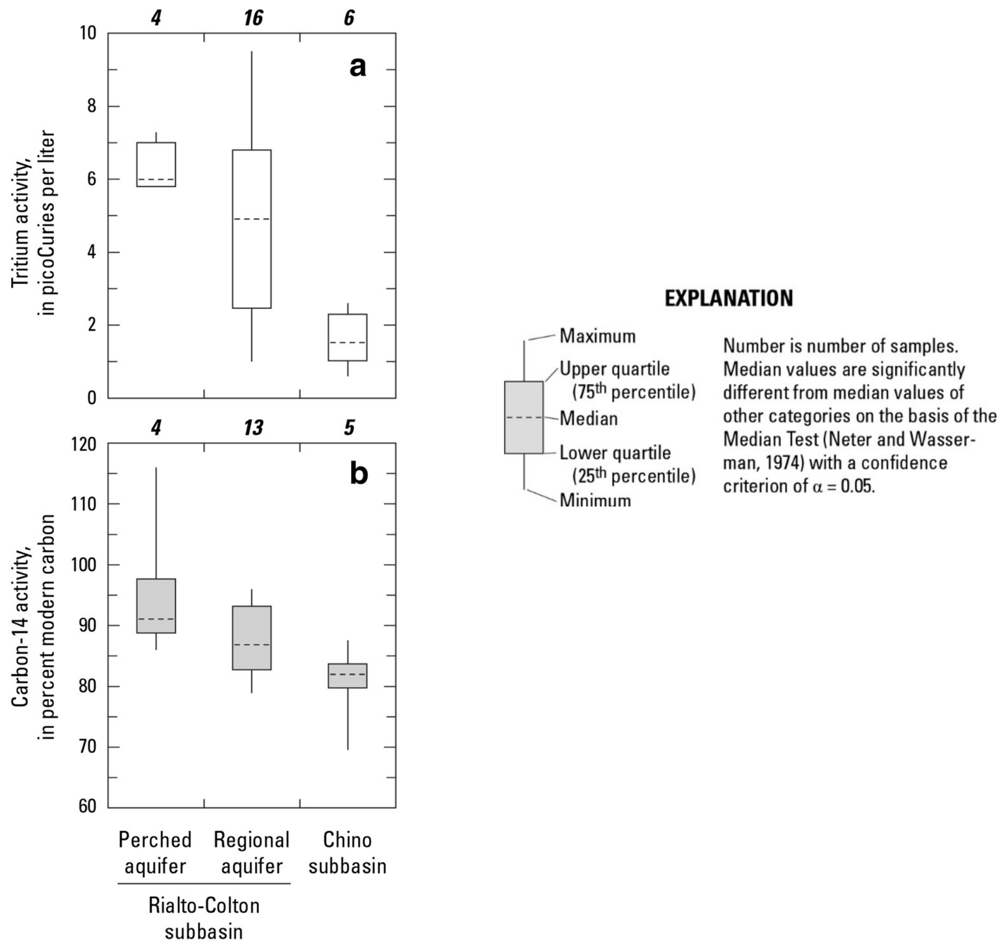

Fig. 14 Ranges in a tritium and b carbon-14 (^{14}C) activities in water from the surface discharge of sampled wells in the perched and regional aquifers within the Rialto-Colton, and Chino groundwater subbasins, California, July 2010 to February 2012

Tritium activities in water from the surface discharge of wells in the Chino subbasin ranged from the reporting level of <0.3 to 2.6 pCi/L (Table S2 of the ESM). Overall, tritium activities were lower in the Chino subbasin than in the perched or regional aquifer within the Rialto-Colton subbasin (Fig. 14). Well F-17B, in the central part of the Chino subbasin, was the only well with a tritium activity less than the detection limit of 0.3 pCi/L, suggesting that water in the well originated as precipitation prior to the atmospheric testing of nuclear weapons beginning in 1952. This is consistent with previous work (Sturchio et al. 2007b) that attributed perchlorate in this well to legacy agricultural land uses occurring prior to 1952.

Carbon-14 is a naturally occurring, radioactive isotope of carbon, having a half-life of about 5,730 years (Mook 1980). Carbon-14 activities are reported as percent modern carbon (pmc), and 13.56 disintegrations per minute per gram of carbon equals 100 pmc (Kalin 2000). Similar to tritium, carbon-14 also was produced as a result of atmospheric testing of nuclear weapons and groundwater containing tritium can have carbon-14 activities greater than 100 pmc. Similar to tritium, carbon-14 also may provide information relevant to the source and occurrence of perchlorate.

Carbon-14 activities from the surface discharge of wells in the Rialto-Colton subbasin ranged from 79 to 116 pmc (Table S2 of the ESM). Carbon-14 activities were higher in the perched aquifer than in the regional aquifer (Fig. 14), and the highest carbon-14 activity was in water from well N-10S (116 pmc) in the perched aquifer. Consistent with tritium data, this high value indicates water from this well was recharged after the onset of atmospheric nuclear weapons testing in 1952 (possibly near the peak of atmospheric testing in 1962); and would coincide with the period of military and industrial activity in the study area that led to the release of perchlorate. The lowest carbon-14 activity in the regional aquifer was in water from well WVWD-11 (79 pmc) near the leading edge of the mapped perchlorate plume. This sample had a tritium activity of 2.1

pCi/L, possibly indicating a fraction of post-bomb water mixed with older water. $\delta^{18}O$ and $\delta^{2}H$ values in water from well WVWD-11 are consistent with higher fractions of water recharged near the mountain front as opposed to Lytle Creek.

Carbon-14 activities from the surface discharge of wells within the Chino subbasin ranged from 70 to 88 pmc (Table S2 of the ESM). Carbon-14 activities were lower in the Chino subbasin, consistent with lower tritium activities and older groundwater ages, than in the perched or regional aquifer within the Rialto-Colton subbasin (Fig. 14). The lowest carbon-14 activity was from well Chino-2. This sample also had relatively low tritium activity (1.1 pCi/L). Similar to water from well WVWD11, these data may indicate a fraction of post-bomb water mixed with older water, and are consistent with lithologic and major-ion data (Fig. 10a), indicating the well is partly completed in the underlying Tertiary-age deposits.

The range in tritium and carbon-14 activities in depth-dependent samples from most sampled wells was small (Table S4 of the ESM). This small range would be expected for wells such as Rialto-6, F-49A and F-17B, having downward flow under unpumped conditions that distributes water from shallower to deeper depths through the well. Well F-10C, which had a complex distribution of upward and downward flow within the well (Figs. 7 and 8), had the largest range in tritium activities (7.1 to <0.3 pCi/L) and carbon-14 activities (90–71 pmc) with depth of any well sampled. Although recent (post-bomb) water was present at shallower depths, the deepest sample (289.6 m below land surface) did not contain measurable tritium and had a carbon-14 activity of 71 pmc (Table S4 of the ESM). These low activities are consistent with major-ion data that show water from partly consolidated Tertiary-age deposits present at depth. Tritium also was not detected in deep samples collected within Rialto-3 (Table S4 of the ESM), although carbon-14 activities did not differ as greatly with depth as in well F-10C. Tritium data are consistent with $\delta^{18}O$ and $\delta^{2}H$ data (Fig. 13b), indicating that water within well Rialto-3 below 228.6 m was recharged near the mountain front that has moved through the aquifer at depth.

Tritium and carbon-14 activities were comparatively uniform with depth in well F-26A, ranging from 2.4 to 2.9 pC/L and 79 to 82 pmc, respectively (Table S4 of the ESM). These data are consistent with at least some recently recharged, post-1952, groundwater throughout the well. Well F-26A penetrates Tertiary-age deposits, and differences in major-ion chemistry (including perchlorate) and age distribution between well F-26A and well F-10C, are consistent with different sources of water to the wells. As previously discussed, upward flow through well F-26A may be driven by aquifers having higher head on the opposite side of the Rialto-Colton Fault (1,200 m east) or Barrier J (3 km to the northwest). In contrast, upward flow at depth below 240 m within well F-10C (Fig. 7) is locally driven by pumping within nearby in well F-10B.

Dissolved gases

Dissolved gases measured as part of this study were argon, nitrogen, and methane (Table S5 of the ESM). Argon, a noble gas, does not react chemically in water. Nitrogen also is relatively non-reactive, but may be produced in groundwater as a result of denitrification under reducing conditions. Argon, nitrogen, and methane occur naturally in the atmosphere and their solubility in water is a function of temperature, pressure, and salinity according to Henry’s Law (Stumm and Morgan 1996). The change in argon and nitrogen gas concentration in pure water at one atmosphere pressure as a function of temperature is shown as the water-air equilibrium line (Fig. 15). Gas concentrations greater than expected according to Henry’s Law occur if infiltrating water traps bubbles of air, known as excess air, that later dissolve (Stute and Schlosser 2000). Argon and nitrogen concentrations in groundwater from excess air increase with respect to the atmospheric concentration of these gases, rather than according to solubility from Henry’s Law (Fig. 15).

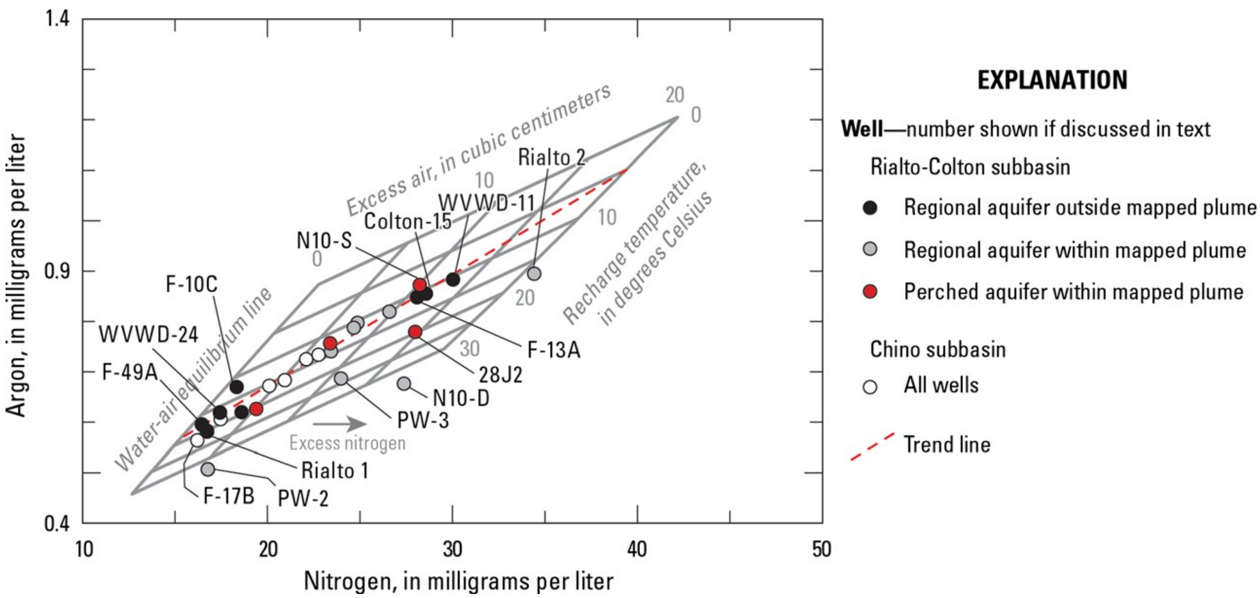

Fig. 15 Nitrogen and argon concentrations in water from sampled wells, in the Rialto-Colton and Chino groundwater subbasins California, 2010 to 2012

The combination of temperature and excess-air effects on dissolved-gas concentrations in groundwater can provide information interpretable in terms of the source and timing (seasonality) of groundwater recharge, and of chemical reactions (such as denitrification) within aquifers. In general, cooler groundwater recharge temperatures and greater excess-air concentrations are consistent with recharge from winter streamflows that infiltrated rapidly through the unsaturated zone (entrapping air). In contrast, warmer groundwater recharge temperatures and lower excess-air concentrations are consistent with recharge from sustained streamflows along losing stream reaches downstream from the mountain front, with areal recharge from precipitation, or irrigation return that infiltrated slowly through the unsaturated zone prior to recharge (Stute and Schlosser 2000).

Recharge temperatures estimated from dissolved argon and nitrogen-gas concentrations in water from most wells in the Rialto-Colton subbasin ranged from about 19 °C, approximately the average annual temperature of the study area, to about 10 °C (Fig. 15). Most samples within the Rialto-Colton subbasin were recharged under cooler-than average annual temperatures, and as recharge temperature decreased excess air increased—consistent with recharge from focused recharge sources such as infiltration of winter streamflows along Lytle Creek. Although streamflow in Lytle Creek infiltrates outside the Rialto-Colton subbasin, it may subsequently move across the San Jacinto Fault and Barrier E into the subbasin as groundwater. The dissolved gas concentrations at the time of recharge are preserved in the groundwater enabling identification of the recharge source.

When interpreted in light of $\delta^{18}O$ and $\delta^{2}H$ data (Fig. 13a), dissolved-gas data (Fig. 15) suggest multiple recharge sources in the Rialto-Colton subbasin that include: (1) recharge from Lytle Creek that infiltrated closer to the mountain front during sustained spring and early summer flows, and consequently has lighter $\delta^{18}O$ and $\delta^{2}H$ values, warmer temperatures and less excess-air than winter stormflows (WVWD-24, Rialto-1), (2) recharge from winter stormflows infiltrated along downstream reaches of Lytle Creek, with lighter $\delta^{18}O$ and $\delta^{2}H$ values, colder recharge temperatures and greater excess air than water infiltrated by sustained streamflow (Colton-15), and (3) mountain front recharge dominated by infiltration of runoff after winter storms, with heavier $\delta^{18}O$ and $\delta^{2}H$ values, colder recharge temperatures and high excess air (F-13A, WVWD-11). As previously discussed, depth-dependent chemical and isotopic data show water from some wells such as Rialto-3 and F-10C, was recharged from different sources entering the well along discrete flowpaths with depth.

In contrast to water from other sampled wells, groundwater temperatures and excess air-values in water from F-10C and F-49A plot close to the water-air equilibrium line (Fig. 15). This may occur because the dissolved gas concentrations in water from these wells were reset by water cascading into the wells.

Water from several wells within the contaminant plume (Rialto-2, 28 J2, N-10D, PW-2, and PW-3) appear to have relatively high nitrogen/argon ratios and an excess of nitrogen gas relative to other wells (Fig. 15). Although native groundwater in the aquifer is generally oxic, and water within the perchlorate plumes also is generally oxic, it is possible that excess-nitrogen gas in these wells could be indicative of denitrification and reducing conditions at some point within the groundwater flow system. Methane indicative of strongly reducing conditions (not shown in Table S5 of the ESM) was only detected in water from Rialto-2 at a concentration of 0.003 mg/L (the methane concentration in Rialto-2 at 243.8 m depth was 0.024 mg/ L). Reducing conditions and potential denitrification in water from wells was evaluated on the basis on nitrate isotope data (discussed later in this report).

In comparison to the Rialto-Colton subbasin, water from wells in the Chino subbasin had higher estimated recharge temperatures and less excess air (Fig. 15). Recharge temperatures closer to the average annual temperature of the study area may indicate a greater fraction of areal recharge within the Chino subbasin compared to the Rialto-Colton subbasin which receives recharge originally infiltrated from stormflows in Lytle Creek that recharged the Rialto-Colton subbasin as groundwater movement across Barrier E and the San Jacinto Fault. Warm recharge temperatures, the small amount of excess air, and δ^{18}O and δ^{2}H data (Fig. 10a) are consistent with irrigation return and partial evaporation of water from well F-17B.

Stable isotope ratios in nitrate and sulfate

Nitrogen, sulfur, and oxygen isotope ratios within nitrate and sulfate ions were measured to determine if the sources of these constituents might be related to different water masses and if microbial reduction of nitrate or sulfate occurred within the aquifer. If reduction of nitrate or sulfate occurred, it is possible that reduction of perchlorate also may have occurred.

The nitrogen isotopic composition of nitrate (δ^{15}N–NO_3) from the surface discharge of most sampled wells ranged from 1.4 to 7.3 ‰, and the oxygen isotopic composition of nitrate (δ18O–NO3) ranged from 4.1 to 8.9 ‰ (Table S2 of the ESM). The ranges in δ^{15}N – NO_3 and δ^{18} – -NO_3 values in the study area are small compared to the ranges reported for natural water (Coplen et al. 2002) and generally consistent with those expected from nitrification of common reduced nitrogen sources including soils, fertilizers, and local organic contaminants (Heaton 1986; Kendall and Aravena 2000; McMahon and Böhlke 2006; Jackson et al. 2010; Andraski et al. 2014). Isotopically heavier values commonly associated with extensive denitrification were not present. In general, nitrate concentrations and δ^{15}N–NO_3 values were greater in the Chino subbasin than in the Rialto-Colton subbasin. δ^{18}O–NO_3 values decreased with increasing δ^{15}N–NO_3 values, consistent with differences in nitrate sources, rather than increasing together consistent with denitrification (Böttcher et al. 1990; Granger et al. 2008; Izbicki 2014). Samples having high nitrogen/argon ratios and excess nitrogen gas, Rialto-2, 28 J2, N-10D, PW-2 and PW-3 (Fig. 15) did not have anomalously elevated δ^{15}N– NO_3 or δ^{18}O–NO_3 values. This could indicate that (1) high nitrogen/argon ratios resulted from some other process, perhaps related to recharge or subsequent degassing, or (2) the samples contained mixtures of undenitrified and denitrified water such as might exist above and below a redox boundary (Böhlke et al. 2007). Water from the WestBay sample port PW-5D had anomalously high δ^{15}N– NO_3 and δ^{18}O–NO_3 values of 19 and 11 ‰, respectively (Table S2 of the ESM). This sample also had an unusual major-ion composition (Fig. 10) and was one of the few wells with detectable nitrite concentrations, 0.78 mg/L as N (not shown in Table S2 of the ESM). These data are consistent with localized partial denitrification in water from PW-5D. It was not possible to measure dissolved gasses in water from the WestBay sample port to provide additional evidence for denitrification. Differences in δ^{15}N– NO_3 and δ^{18}O–NO_3 values with depth in wells F-17B, F-49A, Rialto6, and Rialto-2 were less than 1 ‰ (Table S4 of the ESM) and do not indicate denitrification at depth within the aquifer penetrated by these wells, even though dissolved-oxygen concentrations generally decreased with depth (Table S3 of the ESM). In contrast, δ^{15}N– NO_3 and δ^{18}O–NO_3 values increased by as much as 1.7 and 1.3 ‰ at depth within well F-26 and could indicate potential denitrification, although denitrification at depth within well F-26 was not apparent in dissolved-gas data. Relatively low $\delta^{18}O–NO_3$ values at the two deepest sample depths in water from wells F-10C and Rialto-3 (0.7 to 0.9 ‰, respectively, Table S4 of the ESM) were outside the range of other wells measured in the study area, and are consistent with (1) different geologic conditions at depth in well F-10C indicated by well-bore flow (Fig. 8) and major-ion data (Fig. 10), and 2) different water mass and recharge history for well Rialto-3 indicated by $\delta^{18}O$ and δ_2H data (Fig. Fig. 13). Water from these samples was comparatively old and did not contain reportable tritium.

The sulfur isotopic composition of sulfate ($\delta^{34}S–SO_4$) from the surface discharge of sampled wells ranged from 0.6 to 5.8 ‰, and the oxygen isotopic composition of sulfate ($\delta^{18}O–SO_4$) ranged from 2.9 to 5.2 ‰ (Table S2 of the ESM). The ranges in $\delta^{34}S–SO_4$ and $\delta^{18}O–SO_4$ values are small compared to the ranges reported for natural water (Coplen et al. 2002). There was not a consistent relation between $\delta^{34}S–SO_4$, $\delta^{18}O–SO_4$ and sulfate concentrations, and there was little difference in these constituents between the Rialto-Colton and Chino subbasins or within the mapped plume within the Rialto-Colton subbasin. Despite its unusual major-ion composition, the sulfate concentrations and isotopic composition of water from WestBay sample port PW-5 was within the range of other sampled wells, and did not suggest localized sulfate reduction. Similarly, water from well F-26A did not suggest sulfate reduction at depth. $\delta^{34}S– SO_4$ compositions for water from well F-13A (0.6 ‰, Table S2 of the ESM) and depth-dependent samples collected within wells F-10C and Rialto-3 at 298.6 and 234.7 m below land surface were relatively low (0.3 and −3.7 ‰, respectively; Table S4 of the ESM). Similar to $\delta^{18}O–NO_3$ data, these values were consistent with different geologic conditions, and with different water mass having different recharge histories discussed previously.

Summary and conclusions

Perchlorate from military, industrial, and agricultural sources is present within alluvial aquifers pumped for water supply in the Rialto-Colton groundwater subbasin, 80 km east of Los Angeles, California (USA). The area is extensively faulted and many of the faults are barriers to groundwater flow. Consistent with previous work, the direction of groundwater movement in the regional aquifer within the Rialto-Colton subbasin was from recharge sources near the San Gabriel Mountains toward the southeast, roughly parallel to the faults that bound the subbasin. Interpretation of $\delta^{18}O$, $\delta^{2}H$, and dissolved-gas data show recharge sources include: (1) recharge from Lytle Creek infiltrated closer to the mountain front during sustained spring and early summer flows, (2) recharge from winter stormflows infiltrated along downstream reaches of Lytle Creek, and (3) mountain front recharge dominated by infiltration of runoff from smaller streams.

Flow logs collected within wells under unpumped conditions show downward movement of water through long-screened production wells that may redistribute perchlorate from shallower to deeper deposits within the contaminant plumes at rates as high as 13 kg/year in some wells. This may partly explain the presence of perchlorate in deeper parts of the aquifer that would normally be isolated from surface sources of contamination. Upward flow in a well on the downgradient side of the Rialto-Colton Fault from permeable units within partly consolidated Tertiary-age deposits penetrated by the well may result from a hydraulic connection to aquifers having higher head on the opposite side of the Rialto-Colton Fault (about 1,200 m to the east), or on the opposite side of Barrier J (3 km to the northwest). Given the complex stratigraphy and layering within most alluvial aquifers it may be difficult (or impossible) to identify hydraulically connected layers within alluvial aquifers using commonly available data such as lithologic or geophysical logs. Well-bore flow data from long-screened wells that fully penetrate aquifer deposits may be the only way to identify hydraulically connected layers within aquifers and groundwater flow through those layers across faults.

Flow logs collected within long-screened production wells under pumped conditions show changes in flow consistent with the conceptual understanding of aquifer layering and changes in hydraulic properties throughout the subbasin. Most logs show greater yields to wells from shallower alluvium which contributes as much as 50 % of the flow to some wells. Yields to wells generally decrease with depth. In contrast to lithologic or geophysical logs, pumped flow logs provide direct information on well yield and aquifer hydraulic properties with depth that can be used to further refine conceptual understanding of layering within complex aquifer systems.

For wells having downward flow under unpumped conditions, groundwater chemistry and isotopic compositions were similar at depth within the well as a result of redistribution of shallower groundwater throughout the well. For wells having upward (or near zero) flow under unpumped conditions, differences in groundwater chemistry with depth were interpretable with respect to the source of water and age of water contributing flow to wells. Coupled well-bore flow and depth-dependent water chemistry data indicate that samples from the surface discharge of long-screened production wells, that are mixtures of water from different depths penetrated by the well, may underestimate maximum perchlorate and nitrate concentrations near the water table. Coupled well-bore flow and depth-dependent water-quality data also show reduced conditions at depths penetrated by some wells, but do not show sufficiently reduced conditions to promote reduction of nitrate or sulfate (or by extension perchlorate) at depth where dissolved oxygen concentrations are low.

Hydrologic, water-chemistry, and isotopic data collected as part of this study provide the hydrogeologic context needed to support interpretation of chlorine and oxygen isotopes within perchlorate sampled as part of this study. Water-level data within the perched aquifer suggest some water may move from the Rialto-Colton to the Chino subbasin across the Rialto-Colton Fault through the perched aquifer, and well-bore flow data suggest that some water may move across the Rialto Colton Fault at depth through partly consolidated Tertiary-age deposits. In both cases, the amount of water movement is likely small, and additional data collection and analyses would be required to quantify the rate of water movement. Additional interpretation of the source and movement of perchlorate within the study area will be made on the basis of chlorine and oxygen isotopic data within the context of local geology and hydrologic conditions identified within this study.

Acknowledgements

This work was funded by the United States Department of Defense (DOD) Environmental Security Technology Certification Program (ESTCP). Additional funding was provided cooperatively by the San Bernardino Valley Municipal Water District (SBVMWD) in cooperation with the US Geological Survey (USGS), and by the US Environmental Protection Agency (US EPA). The authors thank local stakeholders, their staff, and their consultants who provided data, access to wells, and input to the project, including review of this manuscript, through the Technical Advisory Committee (TAC). Collection of well-bore flow and depth-dependent water-chemistry data from wells in this study would not have been possible without the support and assistance of Fontana Water District, City of Rialto, County of San Bernardino, and the US EPA.

References

Anderson M, Roberts C, Jachens R (2000) Principal facts for gravity stations in the vicinity of San Bernardino, southern California. US Geol Surv Open File Report 00–193, 32 pp. http://pubs.usgs.gov/of/2000/0193/. Accessed 29 October 2014

Anderson M, Matti J, Jachens R (2004) Structural model of the San Bernardino basin, California, from analysis of gravity, aeromagnetic, and seismicity data. J Geophys Res 109(B04404):1– 20

Andraski BJ, Jackson WA, Welborn TL, Böhlke JK, Sevanthi R, Stonestrom DA (2014) Soil, plant, and terrain effects on natural perchlorate distribution in a desert landscape. J Environ Qual 43:980–994

Belitz K, Hamlin SN, Burton CA, Kent R, Fay RG, Johnson T (2004) Water quality in the Santa Ana Basin, California, 1999– 2001. US Geol Surv Circ File 1238, 37 pp. http://pubs.usgs.gov/circ/2004/1238/pdf/circular1238.pdf. Accessed 29 October 2014

Bense VF, Van Balen RT, DeVries JJ (2003) The impact of faults on the hydrogeological conditions in the Roer Valley Rift System: an overview. Neth J Geosci 82(1):41–54

Böhlke JK, Sturchio NC, Gu B, Horita J, Brown GM, Jackson WA, Batista J, Hatzinger PB (2005) Perchlorate isotope forensics. Anal Chem 77:7838–7842

Böhlke JK, O'Connell ME, Prestegaard KL (2007) Ground-water stratification and delivery of nitrate to an incised stream in varying flow conditions. J Environ Qual 36:664–680

Böhlke JK, Hatzinger PB, Sturchio NC, Gu B, Abbene I, Mroczkowski J (2009) Atacama perchlorate as an agricultural contaminant in groundwater: isotopic and chronological evidence from Long Island, New York. Envron Sci Technol 43(15):5619–5625

Böttcher J, Strebel O, Voerkelius S, Schmidt HL (1990) Using isotope fractionation of nitrate-nitrogen and nitrate oxygen for evaluation of microbial denitrification in a sandy aquifer. J Hydrol 114:413–424

Brandhuber P, Clark S, Morley K (2009) A review of perchlorate occurrence in public drinking water systems. JAWWA 101(11):63–73

Bredehoeft JD, Belitz K, Sharp-Hansen S (1992) The hydrodynamics of the Big Horn Basin: a study of the role of faults. Am Assoc Petrol Geol Bull 76(40):530–546

Caine JS, Minor SA (2009) Structural and geochemical characteristics of faulted sediments and inferences on the role of water in deformation, Rio Grande Rift, New Mexico. Geol Soc Am Bull 121(9/10):1325–1340

Caine JS, Minor SA, Grauch VJS, Hudson MR (2002) Potential for fault zone compartmentalization of groundwater aquifers in poorly lithified, Rio Grande rift-related sediments, New Mexico. Geol Soc Am (Abs) 34(4):59

California Department of Public Health (2007) Perchlorate in drinking water. California Department of Water Resources, Sacramento, CA. http://www.cdph.ca.gov/certlic/drinkingwater/ pages/Perchlorate.aspx. Accessed 8 August 2012

California Department of Water Resources (2004) California's groundwater: Upper Santa Ana Valley groundwater, Rialto-Colton subbasin. Bull. 118, California Department of Water Resources, Sacramento, CA. http://www.water.ca.gov/pubs/ groundwater/bulletin_118/basindescriptions/8-2.04.pdf. Accessed 26 February 2013

Catchings R, Rymer M, Goldman M, Gandhok G, and Steedman C (2008) Structure of the San Bernardino Basin along two seismic transects: Rialto-Colton fault to the San Andreas fault and along the I-215 Freeway (I-10 to SR30). US Geol Surv Open File Report 2008–1197, 70 pp. http://pubs.usgs.gov/of/2008/1197/. Accessed 29 October 2014

CH2M-Hill (2012) Final numerical groundwater flow model report, Rialto-Colton basin. Prepared for the US EPA, CH2M-Hill, Reading, CA, variously paged

Coates JD, Achenbach LA (2004) Microbial perchlorate reduction: rocket-fuelled metabolism. Nat Rev Microbiol 2:569–580

Coplen TB, Hopple JA, Böhlke JK, Peiser HS, Rieder, SE, Krouse HR, Rosman KJR, Ding T, Vocke RD, Revesz KM, Lamberty A, Taylor P, De Bievre P (2002) Compilation of minimum and maximum isotope ratios of selected elements in naturallyoccurring terrestrial materials and reagents. US Geol Surv Water Resour Invest Rep 01–4222, 98 pp. http://pubs.usgs.gov/wri/wri014222/. Accessed 29 October 2014

Craig H (1961) Isotopic variations in natural waters. Science 133:1702–1703

Dafny E, Gvirtzman H, Burg A (2013) Identifying watershed-scale groundwater flow barriers: the Yoqne'am Fault in Israel. Hydrogeol J 21:1035–1051

DPRA Inc (2008) Draft site inspection report: perchlorate, trichloroethene and other hazardous substances with the Rialto-Colton Groundwater basin, County of San Bernardino, CA. DPRA Project no. 004569, DPRA, San Marcos, CA, variously paged

Dutcher L, Garrett A (1963) Geologic and hydrologic features of the San Bernardino area, California: with special reference to underflow across the San Jacinto fault. US Geol Surv Water Supply Pap 1419, 114 pp. http://pubs.er.usgs.gov/publication/ wsp1419. Accessed 29 October 2014

Eckis R (1928) Alluvial fans of the Cucamonga district, southern California. J Geol 36:225–247

Folch A., Mas-Pla J (2008) Hydrogeological interactions between fault zones and alluvial aquifers in regional flow systems. Hydro. Proces. 22:3476–3487

Forster CB, Evans JP (1991) Hydrogeology of thrust faults and crystalline thrust sheets: results of combined field and modeling studies. Geophys Res Lett 18(5):979–982

Fram MS, Belitz K (2011) Probability of detecting perchlorate under natural conditions in deep groundwater in California and the southwestern United States. Environ Sci Technol 45(4):1271–1277. doi:10.1021/es103103p

Freeze RA, Cherry JA (1979) Groundwater. Prentice-Hall, Englewood Cliffs, NJ, 604 pp

GeoLogic Associates (1997) Evaluation monitoring program, Phase I Point-of-Compliance Study, Mid-Valley Sanitary Landfill. Prepared for County of San Bernardino Waste System Division, Geologic, Claremont, CA

GeoLogic Associates (1998) Phase II (Offsite) Evaluation monitoring program, Mid-Valley Sanitary Landfill, County of San Bernardino, California, Anaheim, CA. Geologic, Claremont, CA, variously paged

GeoLogic Associates (2003) Perchlorate Investigation in the Vicinity of the Mid Valley Sanitary Landfill. San Bernardino, California, Anaheim, CA, Geologic, Claremont, CA, variously paged

GeoLogic Associates (2010) Updated hydrogeologic model of perchlorate transport conditions in the northern RCB. San Bernardino County, California, Anaheim, CA, Geologic, Claremont, CA, variously paged

GeoLogic Associates (2013) First quarter (winter) 2013 monitoring report Rialto GWTS perchlorate and VOC investigation, San Bernardino County, California, Anaheim, CA, Geologic, Claremont, CA, variously paged

GeoLogic Associates (2002) Environmental audit, potential sources of perchlorate impacts, Rialto-Colton Groundwater Basin. San Bernardino County, California, Anaheim, CA, Geologic, Claremont, CA, variously paged

GeoSyntec Consultants (2006) Additional interim remedial investigation report. Prepared for Goodrich Corporation, GeoSyntec, Atlanta, GA, 127 pp

Gosling AW (1967) Patterns of subsurface flow in the BloomingtonColton Area Upper Santa Ana Valley, California. US Geol Surv Hydrol Invest Atlas HA-268, 1 map

Government Accountability Office (2010) Perchlorate: occurrence is widespread but at varying levels. 63 pp. http://www.gao.gov/ new.items/d10769.pdf. Accessed 8 August 2012

Granger J, Sigman DM, Lehmann MF, Tortell PD (2008) Nitrogen and oxygen isotope fractionation during dissimilatory nitrate reduction by denitrifying bacteria. Limnol Oceanogr 53:2533–2545

Hatzinger P, Böhlke JK, Sturchio NC, Gu B, Heraty LJ, Borden RC (2009) Fractionation of stable isotopes in perchlorate and nitrate during in situ biodegradation in a sandy aquifer. Environ Chem 6:44–52. http://www.publish.csiro.au/?paper=EN09008. Accessed 29 October 2014

Heaton THE (1986) Isotopic studies of nitrogen pollution in the hydrosphere and atmosphere: a review. Chem Geol 59:87–102

IAEA (1981) Stable isotope hydrology. Technical report series no. 210, Vienna, Austria, International Atomic Energy Agency, Vienna, 339 pp

Izbicki JA (2003) Source and movement of ground water in the western part of the Mojave Desert, southern California, USA. US Geol Surv Water Resour Invest Rep 03–4313, 28 pp. http://pubs.er.usgs.gov/publication/wri034314. Accessed 29 October 2014

Izbicki JA (2004) A small-diameter sample pump for collection of depth-dependent samples from production wells under pumping conditions: US Geol Surv Fact Sheet 2004–3096. http://pubs.usgs.gov/fs/2004/3096/. Accessed 29 October 2014

Izbicki JA (2014) Fate of nutrients in shallow groundwater receiving treated septage, Malibu, CA. Ground Water 52:218– 233. doi 10.1111/gwat.12194/full

Izbicki JA, Danskin WR, Mendez GO (1998) Chemistry and isotopic composition of ground water along a section near the Newmark area, San Bernardino County, California. US Geol Surv Water Resour Invest Rep 97–4179, 27 pp

Izbicki JA, Christensen AH, Hansen RT (1999) U.S. Geological Survey combined well-bore flow and depth-dependent water sampler. US Geol Surv Fact Sheet 196–199, 2 pp. http://ca.water.usgs.gov/archive/reports/fs19699.pdf. Accessed 29 October 2014

Jackson WA, Böhlke J, Gu B, Hatzinger P, Sturchio NC (2010) Stable isotope composition of indigenous natural perchlorate and co-occurring nitrate in the southwestern United States. Environ Sci Technol 44:4869–4876

Kalin RM (2000) Radiocarbon dating of groundwater systems, chap 4. In: Cook PG, Herczeg AL (eds) Environmental tracers in subsurface hydrology. Kluwer, Boston, pp 111–144

Kendall C, Aravena R (2000) Nitrate isotopes in groundwater systems. In: Cook PG, Herczeg AL (eds) Environmental tracers in subsurface hydrology. Kluwer, Boston, pp 261–297

Kent R, Landon MK (2012) Trends in concentrations of nitrate and total dissolved solids in public supply wells of the Bunker Hill, Lytle, Rialto, and Colton groundwater subbasins, San Bernardino County, California: influence of legacy land use. Sci Total Environ 452-453C(2013):125–136

Lieberman MT, Borden RC (2008) Natural attenuation of perchlorate in groundwater processes, tools, and monitoring techniques. ESTCP Project ER-0428, US Dept. of Defense, Washington, DC, 58 pp

Lippincott JB (1902) Development and application of water near San Bernardino, Colton, and Riverside, California. US Geol Surv Water Supply Pap 59, 95 pp

Lu Z, Danskin W (2001) InSAR analysis of natural recharge to define structure of a ground-water basin, San Bernardino, California. Geophys Res Lett 28:2661–2664

McMahon PB, Böhlke JK (2006) Regional patterns in the isotopic composition of natural and anthropogenic nitrate in groundwater, High Plains, USA. Environ Sci Technol 40:2965–2970. doi:10.1021/es052229q

Mook WG (1980) Carbon-14 in hydrogeological studies. In: Fritz P, Fontes JCh (eds) Handbook of environmental isotope geochemistry. Springer, Heidelberg, Germany, pp 49–74

Motzer WE (2001) Perchlorate: problems, detection, and solutions. Environ Forensics 2(4):301–311. doi:10.1006/enfo.2001.0059 Neter J, Wasserman W (1974) Applied linear statistical models. Irwin, Homewood, IL, 842 pp

Paulinski S (2012) Structural, hydrogeologic framework and textural model of the Rialto-Colton basin and the Chino and North Riverside area. MSc Thesis, California State Univ., Sacramento, CA, USA, 171 pp

Rao B, Anderson TA, Orris GJ, Rainwater KA, Rajagopalan S, Sandvig RM, Scanlon BR, Stonestrom DA, Walvoord MA, Jackson WA (2007) Widespread natural perchlorate in unsaturated zones of the southwest United States. Environ Sci Technol 41(13):4522–4528. doi:10.1021/es062853i

Smith LC, Forster C, Evans J (1990) Interaction of fault zones, fluid flow, and heat transfer at the basin scale. Hydrogeol Low-Perm Environ 2:41–67

Stumm W, Morgan JJ (1996) Aquatic chemistry. Wiley, New York, 1022 pp

Sturchio NC, Beloso AD, Böhlke JK, Streger SH, Heraty LJ, Hatzinger PB (2007a) Oxygen and chlorine isotopic fractionation during perchlorate biodegradation: laboratory results and implications for forensics and natural attenuation studies. Environ Sci Technol 41:2796–2802

Sturchio NC, LeClaire JP, Beloso AD, Heraty L, Manning KR, Corsinita PJ (2007b) Use of stable isotopes as a forensic tool to determine sources of perchlorate in groundwater in the Chino basin, California. Groundwater Resources Association of California Symposium: Isotope Methods for Groundwater Investigations. Concord, CA, March 2007, Abstract

Sturchio NC, Caffee M, Beloso AD, Heraty LJ, Böhlke JK, Hatzinger PB, Jackson WA, Gu B, Heikoop JM, Dale M

(2009) Chlorine-36 as a tracer of perchlorate origin. Environ Sci Technol 43:6934–6938

Sturchio NC, Beloso A, Heraty LJ, Wheatcraft S, Schumer R (2014) Isotopic tracing of perchlorate sources in groundwater from Pomona, California. Appl Geochem 43:80–87

Stute M, Schlosser P (2000) Atmospheric noble gases. In: Cook P, Herezeg AL (eds) Environmental tracers in subsurface hydrology. Kluwer, Boston, 529 pp

Teague N, Brown A, Woolfenden L (2014) Geohydrologic and water quality data in the vicinity of the Rialto-Colton Fault, San Bernardino, California. US Geol Surv Data Series 813, 29 pp. http://pubs.er.usgs.gov/publication/ds813. Accessed 29 October 2014

US EPA (2002) Perchlorate environmental contamination: toxicological review and risk characterization. NCEA-1-0503, US EPA, Washington, DC, variously paged. http://cfpub.epa.gov/ncea/cfm/recordisplay.cfm?deid=24002#Download. Accessed 8 August 2012

US EPA (2004) Maximum perchlorate concentrations between January 2003 and August 2004, Rialto-Colton basin, San Bernardino, County, California. US EPA Region 9, San Francisco, CA, 1 map

US EPA (2010) Interim action record of decision: source area operable unit B.F. Goodrich Superfund Site, San Bernardino County, CA. EPA ID: CAN000905945, 30 September 2010. US EPA, Region 9, San Francisco, CA, variously paged. http://yosemite.epa.gov/r9/sfund/r9sfdocw.nsf/3dc283e6c5d6056f88257426007417a2/f03db7a027c1e568882577b4006a02fc!OpenDocument. Accessed 26 February 2013

Wibberley C, Yielding G, DiToro G (2008) Recent advances in the understanding of fault zone internal structure: a review. Geol Soc Lond Spec Publ 299:5–33

Wildermuth Environmental Inc. (2000) Groundwater elevation contours and management zone boundaries in TIN/TDS study,

Fall 1997: phase 2A of the Santa Ana Watershed. Final Technical Memorandum, Wildermuth, Lake Forest, CA, variously paged

Wildermuth Environmental Inc. (2003) Chino basin dry-year program modeling report. Wildermuth, Lake Forest, CA, variously paged

Wisely A, Schmidt D (2010) Deciphering vertical deformation and poroelastic parameters in a tectonically active fault-bounded aquifer using InSAR and well level data, San Bernardino basin, California. Geophys J Int 181:1185–1200

Woolfenden LR (2007) Aquifer susceptibility to perchlorate contamination in a highly urbanized basin. In: Trefry MG (ed) Securing groundwater quality in urban and industrial environments. Proceedings of the International Association of Hydrologic Scientists, Groundwater Quality 2007, Fremantle, Western Australia, Dec. 2–7, IAHS Pub. 324, IAHS, Wallingford, UK, pp 156–161,1 CD-ROM

Woolfenden L, Kadhim D (1997) Geohydrology and water chemistry in the Rialto-Colton Basin, San Bernardino County, California. US Geol Surv Water Resour Invest Rep 97–4012, 101 pp

Woolfenden L, Koczot K (2001) Numerical simulation of groundwater flow and assessment of the effects of artificial recharge in the Rialto-Colton Basin, San Bernardino County, California. US Geol Surv Water Resour Invest Rep 00–4243, 147 pp